

WALKS WITH JUMPS: A NEUROBIOLOGICALLY MOTIVATED CLASS OF PATHS IN THE HYPERBOLIC PLANE

JASON DEBLOIS, EDUARD EINSTEIN, AND JONATHAN D. VICTOR

ABSTRACT. We introduce the notion of a “walk with jumps”, which we conceive as an evolving process in which a point moves in a space (for us, typically \mathbb{H}^2) over time, in a consistent direction and at a consistent speed except that it is interrupted by a finite set of “jumps” in a fixed direction and distance from the walk direction. Our motivation is biological; specifically, to use walks with jumps to encode the activity of a neuron over time (a “spike train”). Because (in \mathbb{H}^2) the walk is built out of a sequence of transformations that do not commute, the walk’s endpoint encodes aspects of the sequence of jump times beyond their total number, but does so incompletely. The main results of the paper use the tools of hyperbolic geometry to give positive and negative answers to the following question: to what extent does the endpoint of a walk with jumps faithfully encode the walk’s sequence of jump times?

1. INTRODUCTION

This paper introduces the notion of a *walk with jumps*, which we conceive as an evolving process in which a point moves in a space (for us, typically \mathbb{H}^2) for a fixed duration, in a consistent direction and at a consistent speed except that it is interrupted by a finite set of stereotyped “jump” events, each of which moves a fixed distance at a fixed angle from the walk direction. The walk’s endpoint encodes partial information about the timing of the jumps, and a main goal here is to offer some precise answers to the question of how it does so.

Our biological motivation, laid out in greater detail in Section 1.1, is to use walks with jumps as a novel abstraction of how a neuron represents information, with the walk itself capturing the neuron’s activity over time, and the walk’s endpoint considered as an invariant of this activity. Since neural activity consists of a stereotyped series of action potentials that differ only in their timing, the action potentials need to correspond to jumps that are identical in angle and size.

While the walk with jumps model may somewhat resemble random walk or random flight models, which are well-studied (see eg. [13]), we believe that this resemblance is largely superficial and this model’s features are substantially different. For instance the fixed jump length and jump angle, choices that follow from the biological motivation, imply that any walk with jumps traces out an *embedded* path in \mathbb{H}^2 that is a quasi-geodesic (by Corollary 4.2 and Proposition 4.11, respectively). Indeed, a primary initial motivation for the model’s construction was to provide a continuous interpolation for collections of paths that traverse edges of a tree, and embedding trees in \mathbb{H}^2 is a natural choice for this purpose. Corollary 5.5 gives an explicit form in which the model successfully accomplishes this goal.

Date: June 25, 2024.

Despite the rigid constraints on the nature of jumps, walks with jumps in \mathbb{H}^2 exhibit a rich collection of behaviors as captured by their endpoints: under broad circumstances, the collection of endpoints is the closure of its interior (Corollary 2.21) and has large diameter (Remark 2.22). This reflects fundamental structural differences between the isometry groups of \mathbb{H}^2 and \mathbb{R}^2 . Unlike in the Euclidean case, where the set of translations forms an abelian normal subgroup, hyperbolic translations do not in general commute, and their product is not necessarily a translation. It is due to this that changing only the *timing* of the jumps—not the angle or length—can profoundly affect the walk with jumps’s endpoint.

Another point of departure from existing mathematical literature is that, in keeping with our biological motivation, we focus on finite-time behavior of walks with jumps (hence a finite number of jumps), rather than their asymptotic behavior, and we make no assumptions about the statistics of the jumps (e.g, whether the intervals are Poisson). In an interval over which information is accumulated to create a percept (typically less than 0.5 sec), a typical neuron may discharge 10 or fewer action potentials, and firing patterns typically differ substantially from Poisson [12].

Ultimately, we are interested in comparing the characteristics of the walks with jumps model to findings in the experimental literature. Here however we focus on establishing basic facts about our construction using classical techniques of hyperbolic geometry and geometric group theory. We now give the formal definition.

Definition 1.1. A **walk with jumps** is specified by the following **initial data**:

- an **origin** $o \in \mathbb{H}^2$, unit tangent vector \mathbf{v} at o , a **walk speed** $s > 0$, **jump angle** $\theta \in (-\pi, \pi)$, and **jump length** $\ell > 0$;

And the following **jump data**:

- a **duration** $T > 0$, sequence (t_1, \dots, t_n) of **jump times** ($n \geq 0$), where

$$0 \leq t_1 < \dots < t_n \leq T,$$

and a **burst vector** (j_1, \dots, j_n) with natural number entries, taken to be $(1, \dots, 1)$ if not otherwise specified.

The walk’s **number of jumps** is $N = \sum_{i=1}^n j_i$; we also call it a **walk with N jumps**.

This data encodes the following set of instructions for movement:

Beginning at o , walk along the geodesic ray in the direction of \mathbf{v} at speed s until time t_1 . At time t_1 , instantly jump a distance of $\ell \cdot j_1$ along an axis through the current location at a counterclockwise angle of θ to the original; then proceed at speed s along a geodesic ray at angle $-\theta$ to the jump axis. Continue until time t_2 ; jump a distance $\ell \cdot j_2$ along an axis at angle θ to the current one; then proceed right again along an axis at angle $-\theta$ to the jump axis, etc.

Having executed the instructions above and halted at time T , our avatar’s final location is the **endpoint** of the walk with jumps. It carries the initial tangent vector \mathbf{v} with it by parallel transport, finally yielding a tangent vector at the endpoint which we call the **endvector**.

Remark 1.2. In Definition 1.1, we choose to use burst vectors to encode multiple jumps at a single time rather than allowing consecutive jump times to be equal.

While these two different approaches are equivalent, using burst vectors will be technically convenient when we write walks with jumps as words in isometries of \mathbb{H}^2 specified by the data $o, \mathbf{v}, s, \theta, \ell$ and T , see Section 2.1.

The central question of this paper is of the extent to which the jump data of a walk with jumps can be recovered from its endpoint p , or the finer information (p, \mathbf{w}) , where $\mathbf{w} \in T_p\mathbb{H}^2$ is the endvector, for a fixed set of initial data. We offer a spectrum of partial answers to this question in Sections 2, 3 and 4, in both positive and negative directions, reflecting the truism that hyperbolic space is “Euclidean at small scales and treelike at large scales”. What this should mean for walks with jumps is fleshed out in Section 1.2. We show there that for the analog of a walk with jumps construction in the Euclidean plane, the endpoint is determined solely by the duration and number of jumps. In contrast, for the analogous construction in a tree, any two distinct jump *patterns* produce distinct endpoints.

Section 2 develops calculus tools for understanding how perturbations of a walk’s jump times affect its endpoint-endvector pair. In Section 2.1 we prove Lemma 2.7, a basic fact describing how the data of a walk with jumps uniquely prescribes an isometry carrying its origin-initial vector pair (o, \mathbf{v}) to (p, \mathbf{w}) . Using this we define a differentiable map whose domain is a simplex T_k encoding all walks with k jumps and a fixed duration that share initial data, and whose target space is $\mathrm{SL}_2(\mathbb{R})$, viewed as (a double cover of) the unit tangent bundle of \mathbb{H}^2 .

The main technical result of Section 2, Proposition 2.17 shows that the derivative of this map has full rank on a dense open subset U of T_k for all $k \geq 3$, provided the jump angle θ is at most $\pi/2$. Several Corollaries follow, including 2.20 which asserts that for $k > 3$, if a walk’s sequence of jump times lies in U then there exist arbitrarily small perturbations of this sequence yielding walks with jumps sharing its endpoint and endvector. Corollary 2.21 asserts that for $k \geq 3$, the set of endpoints of walks with jumps is the closure of its interior in \mathbb{H}^2 .

In Section 3 we move beyond perturbations, constructing walks with significantly different jump patterns that still share an endpoint-endvector pair. Proposition 3.5 describes such pairs sharing the same initial data, number of jumps, and duration, but with arbitrarily large gaps between jump times of the first and the second. This construction does rely, however, on there being not too large a gap between the first jump times of the two walks with jumps. In Section 5 we give conditions that eliminate this possibility.

But first, in Section 4 we establish some basic structure results by applying the tools of hyperbolic geometry to a class of paths associated to walks with jumps.

Definition 1.3. For a walk with jumps with the data of Definition 1.1, the associated **walk-with-jumps path** is the broken geodesic in \mathbb{H}^2 obtained by joining the origin o to the pre-jump location p_1 at time t_1 ; joining p_1 to the post-jump location q_1 at time t_1 ; then joining q_1 to the pre-jump location p_2 at time t_2 and so on. Its i th **walk segment** joins q_{i-1} to p_i (or o to p_i , if $i = 1$, or q_n to the endpoint, if $i = n+1$), and its i th **jump segment** joins p_i to q_i . We parametrize it continuously on $[0, sT + \ell \cdot \sum_{i=1}^n j_i]$, mapping 0 to o , by parametrizing each geodesic segment in turn by arclength.

A quick inductive argument shows that the pre- and post-jump locations p_i and q_i at time t_i occur at parameter values $st_i + \ell \sum_{k=1}^{i-1} j_k$ and $st_i + \ell \sum_{k=1}^i j_k$, respectively, for $i \in \{1, \dots, n\}$.

Remark 1.4. *The endpoints of the walk-with-jumps path associated to a walk with jumps are the origin o and the endpoint of the walk with jumps itself, as defined above. Moreover, its endvector is the outward-pointing unit tangent vector to the final segment of the walk-with-jumps path or, if the final jump time t_n equals T , the unit tangent vector at an angle of $-\theta$ from that vector.*

In Section 4.1 we lay the groundwork for our further results by associating two collections of pairwise disjoint geodesics, the *walk* and *jump axes*, to each walk with jumps. The main result of the subsequent Section 4.2, Proposition 4.11 asserts that any walk-with-jumps path is a *quasi-geodesic*, meaning the hyperbolic distance between any two points on it is well-approximated by their distance along the path (see Definition 4.7). This implies that walks with the same duration but different enough numbers of jumps have different endpoints, see Corollary 4.13.

The main result of Section 5 shows that a pair of conditions, which we now define, ensures that distinct walks with jumps have different endpoints.

Definition 1.5. For $\epsilon > 0$, two walks with jumps sharing initial data and a duration $T > 0$ are *distinct to resolution ϵ* if their sequences of jump times (s_1, \dots, s_m) and (t_1, \dots, t_n) satisfy:

- (1) for each $i \leq \min\{m, n\}$, either $s_i = t_i$ or $|s_i - t_i| > \epsilon$; and
- (2) there exists some i such that $s_i \neq t_i$, or $m \neq n$.

For $R_{\min} > 0$, a walk with jumps has *minimum refractory length R_{\min}* if its burst vector is $(1, \dots, 1)$ —ie. it has no bursts—and for $i \neq j$, $|t_i - t_j| \geq R_{\min}$.

While these conditions may not appear geometrically natural, they are meaningful in biological contexts in which it is not possible to discern differences at arbitrarily small resolutions, and in which physical constraints prevent a neuron from firing again too soon after it has fired once. At suitable scales, they prohibit distinct walks with jumps from having the same endpoint.

Theorem 1.6. *Given $R_{\min} > 0$, the initial data $(o, \mathbf{v}, s, \theta = \pi/2, \ell)$ of a walk with jumps, and a duration $T > 0$, let*

$$\epsilon = \frac{1}{s} \cosh^{-1} \left(\frac{\cosh(sR_{\min}) + 1}{\cosh(sR_{\min}) - \tanh^2 \ell} \right).$$

Any two walks with jumps having the given initial data, duration T , and minimum refractory length R_{\min} that are distinct to resolution ϵ , have distinct endpoints.

Note that for any fixed positive s and ℓ , ϵ defined as above can be made arbitrarily small by choosing R_{\min} large enough. We prove a stronger version of Theorem 1.6 in Section 5 as Theorem 5.4. This more precise version also yields Corollary 5.5, on the existence of trees whose edges are traversed by walk-with-jumps paths.

Section 6 lists further questions, including some that are biologically motivated and others motivated by the hyperbolic-geometric phenomenon called *quasi-geodesic stability*, see Proposition 6.1.

Acknowledgements. JD and EE gratefully acknowledge support from the Swartz Foundation during the initial phase of this work. JDV is supported by NIH EY07977 and NSF 2014217. We thank H. Anuradha Ekanayake, Arshia Gharagozlou, and Mark Fincher for helpful conversations, and Mark for supplying Figures 1, 2, and 3.

1.1. Biological Motivation. We are proposing the walks-with-jumps model as a theoretical framework for modeling neural activity and how it evolves in time. Standard approaches assume (often implicitly) that this evolution occurs in a space with an underlying Euclidean geometry; the material here provides a foundation for replacing this space by a hyperbolic one.

As is standard, we idealize the activity of a single neuron during a time interval as a sample drawn from a point process, i.e., a sequence of stereotyped electrophysiological events (action potentials) which together constitute a “spike train”.

Definition 1.7. Let $t \in \mathbb{R}^+$ and let $k \in \mathbb{N}$. A **spike train (over the period $[0, t]$) with k spikes** is a sequence $t_1 \leq t_2 \leq t_3 \leq t_4 \leq \dots \leq t_k$ with each $t_i \in [0, t]$. We say that **its spikes occur** at the times t_i .

That is, a neuron producing the above spike train has spikes at the times t_i and is quiescent over the periods from t_i to t_{i+1} for each $0 \leq i \leq k - 1$. In our model, the information represented by the neuron over the time interval $[0, t]$ is fully contained in its set of spike times.

Remark 1.8. *Some neurons exhibit bursts: sequences of spikes in very short succession. In the limit of a vanishingly small interspike interval, we can model a burst as a single spike with a magnitude that is a natural number multiple of the stereotypical spike’s.*

A neuron’s activity influences and is influenced by that of others in its network. A central challenge of systems neuroscience is to understand and model how the aggregate activity of a network of such neurons performs cognitive tasks, such as representing the external world or making decisions. Here, we are motivated by considerations about how the activity of individual neurons may contribute to these processes. For example, we can ask the following fundamental question: what way of viewing a spike train captures the “right” amount and quality of information processed by the neuron? An intuitive constraint on the answer is the fact that neural activity is a biological process involving some level of noise and imprecision, so for instance a small variation in the exact timing of its spikes should result in a small change in what this activity represents.

An important stepping stone for pursuing this question is the notion of a “perceptual space” [21] – a mathematical object capturing the mind’s internal representation of a sensory domain, whose structure (e.g. topological, metric, or linear) reflects subjective notions of similarity and difference.

A classic example is the perceptual space of color [21]. It is well-established that for (non-colorblind) humans, this is a three-parameter space [10]. More specifically, colors may be described in terms of real-valued coordinates along three “cardinal” perceptual axes – black vs. white, red vs. green, and blue vs. yellow. To the extent that this space can be regarded as Euclidean – which is clearly an approximation – there is a reasonably satisfying understanding of how it is represented by neural activity (we omit many interesting and important physiological details here; see [3, 18]). In brief, light is transformed into neural signals by three types of photoreceptors, each with its own wavelength-dependent sensitivity to light. Subsequently, neural circuitry in the eye and brain recombines these signals in a way that is, to a first approximation, linear. This leads to coordinates which, while not directly corresponding to the three cardinal axes, can be thought of as a different basis set for the same Euclidean space. With these ingredients, it is straightforward to see

how spike trains could represent the perceptual space of color: it suffices to postulate that neurons correspond to axes in a three-dimensional space, and the total number of spikes within a time interval is the coordinate value represented by a neuron.

Note that in the model above for the color vision perceptual space, the useful information content of a neuron’s activity is entirely captured by a coarse invariant of its spike train, the total spike number. We take this to reflect that space’s relatively simple structure. However, other perceptual spaces appear to be qualitatively different, and the relationship between their structure and the underlying neural activity is much less clear.

A key motivating example for this paper is the human olfactory system. Here there are several hundred kinds of receptors [6], in contrast to the three kinds of receptors relevant to color vision. Furthermore, the perceptual space of odors likely has intrinsically non-Euclidean geometry [22]. So the idea that spike counts behave like Euclidean coordinates, although sufficient to account for how the perceptual space of color might be represented, is likely inadequate to capture the olfactory perceptual space’s complexity.

A simple but important elaboration on this picture is that additional information is contained in the timing of individual spikes. Many experimental studies have shown that this is the case, e.g., [9, 15, 16]. To formalize this idea, a spike train can be represented as a counting process, i.e., a path in which time without a spike consists of movement in one direction, and a spike event corresponds to a jump in a different direction, see e.g. Figure 1. Two spike trains then convey similar messages when their paths are similar. Most often, similarity of spike trains is assumed to be computed by embedding them in a vector space and computing the Euclidean distance between them [16], or, via a “spike time” metric. The latter is an “edit-length distance” [17] given by the minimum “cost” to morph one spike train into another by inserting or deleting spikes, or shifting them in time [19].

However, merely taking spike timing into account does not solve the problem of representing a perceptual space with hyperbolic characteristics. This is because even though the spike time distances are non-Euclidean [1], they (as well as distances derived from vector-spaces) obey a superposition property: using $+$ to denote superposition of spike trains, $D(A, B) = D(A + X, B + X)$. Specifically, inserting a spike at a fixed time to both spike trains will not change the distance between them.

Thus, to be able to capture the hyperbolic geometry that appears to characterize some perceptual spaces, a further generalization is needed. This is our walk-with-jumps model (Figure 1C): spike trains are represented by a path that evolves in time, but the two motions corresponding to time without a spike, and the presence of a spike, are isometries in \mathbb{H}^2 . Note that, because of the non-commutativity of isometries in \mathbb{H}^2 , the superposition property no longer holds. Moreover, the endpoint of a path in \mathbb{H}^2 depends not only on the number of spikes, but also on their arrangement in time. We elaborate on this below.

A separate biological motivation for the walk-with-jumps model is that it provides a new way of viewing the neural substrate of decision-making. There are currently two main conceptual frameworks for this. One is that competing populations of neurons accumulate evidence (i.e., spikes), until one of them reaches a threshold [5]. A second framework views neural population activity as a dynamical

system whose evolution in time is determined by interactions of excitatory and inhibitory neural signals. In this view, decision-making corresponds to entry into an attractor’s basin, from which there is no return [20]. Here, we note that if neural activity evolves in \mathbb{H}^2 , then a “point-of-no-return“ property means that such decisions can result merely from the intrinsic geometry of the space in which neural activity evolves. As we show in Theorem 1.6, this behavior is typical of walks with jumps in \mathbb{H}^2 : if two walks with jumps are sufficiently different up to some time point, then future extensions of them cannot intersect.

Finally, we note that the geometry of \mathbb{H}^2 ensures that the dynamics of the walks-with-jumps model has tree-like features. First, the volume of potential endpoints grows exponentially as a function of the distance from the origin. While the continuous nature of the model will accommodate noise in the exact timing of the spikes, any significant local deviations in the timings of the spikes will lead to walks-with-jumps paths with very different endpoints. This tree-like behavior is natural for modeling the coarse-to-fine characteristics of visual perception [8], as well as perceptual spaces with semantic content.

1.2. Comparing models of a single neuron’s activity.

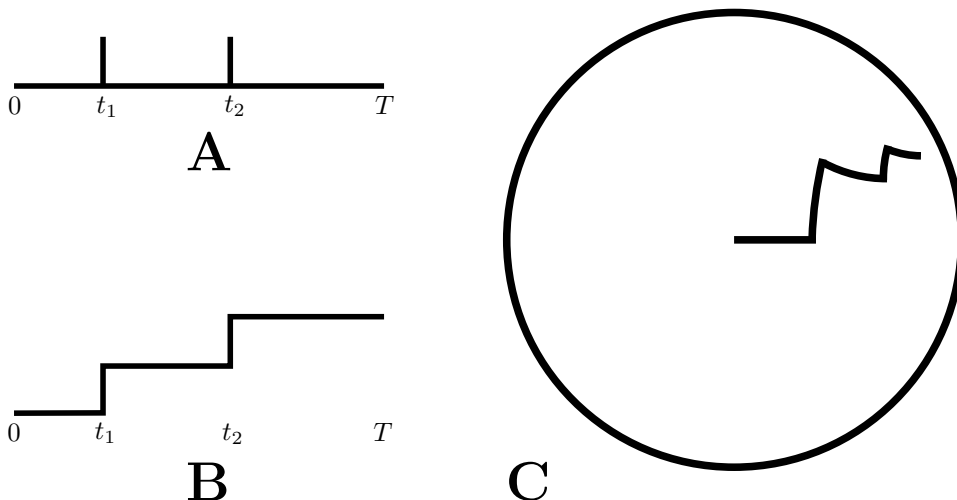


FIGURE 1. This figure shows three different ways of visualizing a spike train.

Figure 1A is a standard conceptualization of a neuron’s activity over a time period $[0, T]$, during which it fires spikes at $t_1 < t_2 < T$ (as defined in 1.7). An equivalent conceptualization is shown in Figure 1B: activity is represented by the counting process $F(t)$, where $F(t) = \int_0^t f(s) ds$ and $f(t)$ is a sequence of (unit-mass) delta-functions corresponding to the point process schematized in Figure 1A.

This second conceptualization has another interpretation: the neuron’s activity is motion of a point along a path in \mathbb{R}^2 , in which the point moves in one direction at constant speed when there is no spike, and then abruptly jumps in another (orthogonal) direction at the times that a spike occurs.

That is, Figure 1B conceptualizes a neuron’s activity as a “walk with jumps”, as in Definition 1.1 but in \mathbb{R}^2 not \mathbb{H}^2 , with origin $(0, 0)$, unit tangent vector $(1, 0)$,

walk speed 1, jump angle $\pi/2$, duration T , and jump length M . For comparison, Figure 1C shows the walk with jumps with the same data, but in \mathbb{H}^2 .

In this section we compare and contrast qualitative features of “walk with jumps” style constructions in various metric contexts, beginning below with that of \mathbb{R}^2 . As we will show, for trajectories in \mathbb{R}^2 , the endpoint is determined solely by the number of spikes and the time interval. That is, two spike trains with the same endpoint can have very different firing patterns. However, in \mathbb{H}^2 , the arrangement of the spikes also influences the endpoint – a feature that is appealing from the point of view that in neural circuits, spike timing, as well as spike count, conveys information. Our overall focus is on the relationship between the endpoint and the path, for example, to what extent do spike trains with the same endpoint necessarily have similar paths?

Example 1.9. *Consider a walk with jumps as in Definition 1.1, but in \mathbb{R}^2 not \mathbb{H}^2 , with origin $(0,0)$, unit tangent vector $(1,0)$, walk speed 1, jump angle $\pi/2$, jump length 1, duration T , and jump times $0 \leq t_1 \leq t_2 \leq \dots \leq t_k \leq T$. Observe that the corresponding walks with jumps path has endpoint:*

$$(T, k) = (t_1, 0) + \sum_{i=1}^k ((t_{i+1} - t_i), 1) + (T - t_k, 0)$$

That is, the path’s endpoint is determined entirely by the walk’s duration and number of spikes.

In Example 1.9, the walk path endpoints do not take into account the timing of individual spikes in a spike train. In contrast, spike timing does affect path endpoints for walks with jumps in \mathbb{H}^2 . The result below uses hyperbolic trigonometry to quantify the effect produced by changing the timing of a single spike, when the jump angle is $\pi/2$. In fact we show that if two such walks have a large enough gap in the timing of their first spikes, then they can never have the same endpoint.

Proposition 1.10. *Consider two walks with jumps in \mathbb{H}^2 , sharing initial data o , \mathbf{v} , s , jump angle $\theta = \pi/2$, and jump length $\ell > 0$. If each walk has a single jump, and this occurs at time 0 in the first and at time T in the second, then the distance d between the two walks’ endpoints satisfies:*

$$\cosh(d) - 1 = (\cosh(\ell) - 1)(\cosh(sT) - 1)(\cosh(\ell) \cosh(sT) - 1).$$

Regardless of how many jumps each has, if the first walk has its first jump at time 0 and the second has its first jump at time t_1 satisfying

$$\sinh(\ell) \sinh(st_1) \geq 1,$$

then the two walks have distinct endpoints.

Proof. The union of walks-with-jumps paths (in the sense of Definition 1.3) for the first two walks considered here (having one jump each) is pictured in Figure 2, using the Poincaré disk model with o at the origin. The vertical line segment in the Figure is the first walk’s jump segment, which has length ℓ in \mathbb{H}^2 . The horizontal line segment is the second walk’s walk segment, of length sT . The other two segments are each contained in circular arcs meeting the unit circle perpendicularly—the form of any hyperbolic geodesic not containing the origin in the Poincaré disk model.

Let q_1 be the far endpoint from o of the first walk’s jump segment, at the top left corner of the shape made by the walk-with-jumps paths of Figure 2, and let p'_1 be

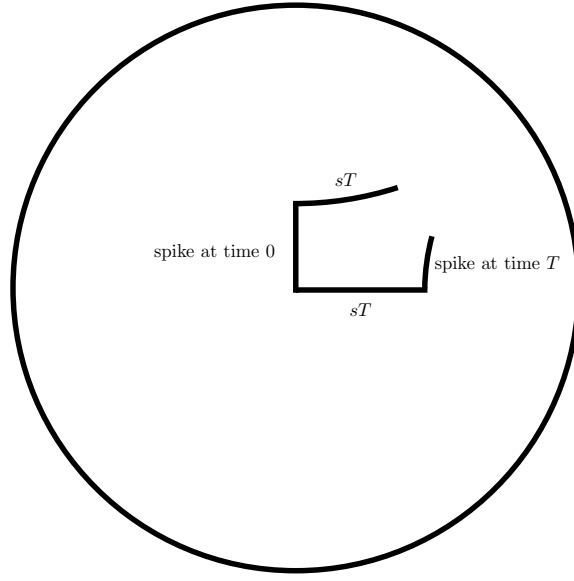


FIGURE 2. This figure shows two hyperbolic walks with jumps over the same time period, T , with a single jump. In one walk, the jump occurs at the beginning of the time period, and in the other it occurs at the end.

the far endpoint from o of the second walk's walk segment. The shortest arc joining the first walk's endpoint to the hyperbolic geodesic containing the second walk's walk segment meets that segment at an angle of $\pi/2$ at a point p'_0 , and therefore defines a *Lambert quadrilateral* Q —one with three right angles—whose vertices are o , q_1 , p'_0 , and the first walk's endpoint.

The first walk's jump segment is one side of Q , of length ℓ , and its walk segment is another, of length sT . Let x be the length of the side of Q joining o to p'_0 , y the distance from the first walk's endpoint to p'_0 , and γ the interior angle at the first walk's endpoint. A hyperbolic law of cosines for Lambert quadrilaterals gives:

$$(1) \quad \sinh(\ell) \sinh(x) = \cos(\gamma).$$

See Theorem 3.5.9 of [14]. A law of cosines for more general quadrilaterals having right angles at two adjacent vertices, recorded as [14, Th. 3.5.8], specializes in the case of Q to give $\cosh(sT) \sin(\gamma) = \cosh(x)$. Using the first equation to replace $\sin(\gamma)$ in the second, and solving for $\sinh(x)$, yields the formula below:

$$\sinh(x) = \frac{\sinh(sT)}{\sqrt{\cosh^2(sT) \sinh^2(\ell) + 1}}.$$

This implies in particular that $x < sT$. Section VI.3.3 of [4] gives several more trigonometric formulas for these more general quadrilaterals. One with the form of a hyperbolic law of sines specializes to $\sinh(y) = \cosh(sT) \sinh(\ell)$ for Q . We apply a final formula from [4] to another such quadrilateral, this one with vertices at the first and second walks' endpoints, and at p'_0 and p'_1 . It gives:

$$\cosh(d) = -\sinh(y) \sinh(\ell) + \cosh(y) \cosh(\ell) \cosh(sT - x).$$

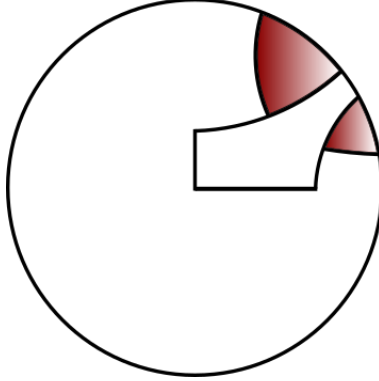


FIGURE 3. Disjoint future quadrants.

The Proposition’s first conclusion is obtained by substituting for x and y in this formula using those obtained above, and simplifying.

We now consider the second situation contemplated in the Proposition, in which both walks may have many jumps but the first walk still has its first jump at time 0. As in the previous case, let q_1 be the far endpoint from o of the first walk’s jump segment, and let p'_1 be the far endpoint of the second walk’s first walk segment. The distance from o to q'_1 is again ℓ , and in this case from o to p'_1 is st_1 .

The geodesic ray from q_1 that contains the first walk’s next walk segment is at a right angle to its first jump segment; and likewise, the geodesic ray containing the second walk’s first jump segment is at right angles to its first walk segment. If these rays intersect, then their subsegments joining q_1 and p'_1 to the point of intersection form a Lambert quadrilateral, together with the first walk’s first jump segment and the second walk’s first walk segment. If so then by the law of cosines for Lambert quadrilaterals, as in (1) above, we would have $\sinh(\ell) \sinh(st_1) = \cos(\gamma)$, where γ is the angle at which the rays meet.

Thus if $\sinh(\ell) \sinh(st_1) \geq 1$ then the two geodesic rays do not intersect. In this case we can deduce that the walks will not share endpoints, since the first walk’s endpoint is on the other side from o of the geodesic containing the ray from q_1 , and the second walk’s endpoint is on the other side from o of the geodesic containing the ray from p'_1 . (We will prove this in Lemma 4.5 below.) \square

The train of thought that finishes off the proof above motivates the notion of “future quadrant”, an intersection of half-planes associated to an initial segment of a walk with jumps that is guaranteed to contain the walk’s endpoint. This is formally defined in Definition 4.6. See Figure 3 for the picture relevant to the proof of Proposition 1.10.

The behavior described in Proposition 1.10 is reminiscent of paths in a tree, which, once they diverge, can never come back together. Another motivating example for the walk with jumps construction is a strategy for encoding a(n approximation to a) spike train by a walk in a tree, as we now describe.

Given a spike train S over a time period t , we can encode a discrete approximation to S in a binary sequence w of length n as follows: for each $1 \leq i \leq n$, if S has a spike in $[(\frac{i-1}{n})t, (\frac{i}{n})t]$, then i th entry of w is 1. If there is no spike in $[(\frac{i-1}{n})t, (\frac{i}{n})t]$,

then the i th entry of w is 0. We can view these discrete approximations of spike trains geometrically by embedding them in a binary tree:

Example 1.11. *Let \mathcal{T} be a binary tree with root p_0 . A binary sequence of length n , $w = w_1 w_2 \dots w_n$ where $w_i \in \{0, 1\}$, encodes a path of length n from p_0 to a vertex of \mathcal{T} as follows: at the root proceed left if $w_1 = 1$ and right if $w_1 = 0$. At the $(i - 1)$ th vertex of the path, proceed left if $w_i = 1$ or right if $w_i = 0$.*

If γ, σ are paths (encoded as binary sequences) of length m, n respectively, then the distance between their endpoints can be computed as follows: if $\gamma = \gamma_1 \gamma_2 \dots \gamma_m$ and $\sigma = \sigma_1 \sigma_2 \dots \sigma_n$, let d be the length of the maximal common prefix of γ and σ . Then the distance between the endpoints of σ and γ is equal to $(m - d) + (n - d)$.

Walks-with-jumps paths in \mathbb{H}^2 have geometry similar to the paths encoded by binary sequences in Example 1.11 with some distinct advantages. First, walks-with-jumps paths can model continuous processes. In the tree T , the binary sequences

$$LRLLLLLLLLLLLLLLL \quad \text{and} \quad LLLLLLLLLLLLLLLLLL$$

are quite similar, but their endpoints will be far apart. The walks-with-jumps model has the feature that non-identical paths that can track each other closely if the event times are similar—behavior that is biologically appealing, since the underlying biophysics of neuronal activity necessarily places a limit on the precision of spike times. This feature more effectively accounts for noise that appears in data.

2. DISTINCT WALKS WITH IDENTICAL ENDPOINTS

In the final section we will produce a fairly general set of conditions in which two walks with jumps are guaranteed to have distinct endpoints, suggesting that to some extent, the endpoint “encodes” the times of the jumps. But first, here, we show that this encoding is not fully faithful. In Section 2.2 we show this via a general but non-constructive argument that implies coincident endpoints for walks with jumps whose jump times are not very different; following that, in Section 3, we create explicit examples of walks with jumps that have distinct jump times but reach the same endpoint, and the jump times of these walks can differ substantially.

2.1. Background and set-up. Standard facts about the geometry of \mathbb{H}^2 imply the following:

Lemma 2.1. *The initial data o, \mathbf{v}, s, θ , and ℓ of a walk with jumps, as in Definition 1.1, determine hyperbolic isometries $f \in \text{PSL}_2(\mathbb{R})$ and the one-parameter family $(g_t)_{t \in \mathbb{R}} \subset \text{PSL}_2(\mathbb{R})$ with the following properties:*

- *The g_t share an axis γ_g through o in the direction of \mathbf{v} , and for each t , g_t translates o a distance of st along γ_g .*
- *The axis λ_f of f contains o , and f translates the origin o a distance of ℓ along λ_f at an angle of θ counterclockwise from γ_g .*

Remark 2.2. *Some remarks about Lemma 2.1:*

- *The initial data of the walk with jumps is recovered from f and the g_t as follows: $o = \lambda_f \cap \gamma_g$, $\frac{d}{dt} \Big|_{t=0} g_t(o) = s\mathbf{v}$, $\ell = d(o, f(o))$, and θ is the counterclockwise angle from \mathbf{v} to the direction vector from o to $f(o)$.*
- *By replacing f and (g_t) with isometries of \mathbb{H}^2 that do not satisfy all requirements of Lemma 2.1, we can produce “walks with jumps” satisfying*

different specifications — for instance with travel along horocyclic arcs or geodesic equidistants.

Definition 2.3. Let w be a word on $\{f, g_t : t \in \mathbb{R}^{\geq 0}\}$. The **syllable length** of w is the smallest number $m \geq 1$ so that w can be grouped as

$$(2) \quad w = g_{s_1} f^{n_2} g_{s_3} f^{n_4} \dots f^{n_{m-1}} g_{s_m}.$$

where $n_i \in \mathbb{Z}^{>0}$ and $s_i > 0$ for $1 < i < m$. We call each of the f^{n_i}, g_{s_i} **syllables** of w . We say w is written in **syllabic form** if expressed as in (2).

We will henceforth abuse notation and use a word w in syllabic form to refer to both the word itself and the isometry that it represents.

Remark 2.4. *The syllabic form of a word should always have an odd number of syllables where the first and last syllables are g_{s_0} and g_{s_m} (which may be the identity). The intermediate syllables cannot be the identity.*

Example 2.5. *The syllable length of $w_1 = g_6 f^2 g_2 g_3 f^3 f$ is 5 because we rewrite w_1 in syllabic form as $g_6 f^2 g_5 f^4 g_0$. The first syllable of the syllabic form is g_6 , the second syllable is f^2 and the third syllable is g_5 .*

Definition 2.6. For a walk with jumps specified by $o, \mathbf{v}, s, \theta, \ell, T, (t_1, \dots, t_n), (j_1, \dots, j_n)$, taking f and $\{g_t\}_{t \in \mathbb{R}}$ as in Lemma 2.1, let

$$w = g_{t_1} f^{j_1} g_{t_2 - t_1} f^{j_2} \dots g_{t_n - t_{n-1}} f^{j_n} g_{T - t_n}.$$

Let w_0 be the identity, $w_1 = g_{t_1}$ and for all $1 \leq i \leq |w|$, let w_i be the product of the first i syllables of w . The *walk axes* are the geodesics $\gamma_i \doteq w_{2(i-1)}(\gamma_g)$ for $i \in \{1, \dots, n+1\}$, and the *jump axes* are the geodesics $\lambda_i \doteq w_{2i-1}(\lambda_f)$ for $i \in \{1, \dots, n\}$, where γ_g, λ_f are as in Lemma 2.1.

Lemma 2.7. *For the walk with jumps specified by initial data $o, \mathbf{v}, s, \theta, \ell$, and jump data $T, (t_1, \dots, t_n)$, and (j_1, j_2, \dots, j_n) , the endpoint-endvector pair is $(w(o), w_*(\mathbf{v}))$, where w from Definition 2.6 is regarded as an isometry of \mathbb{H}^2 , and w_* is its derivative at o . Moreover, for each $i \in \{1, \dots, n+1\}$, γ_i from Definition 2.6 contains the i th walk segment of the associated walk-with-jumps path, as described in Definition 1.3, and λ_i contains the i th jump segment for $i \leq n$.*

Proof. The proof proceeds by induction on n . In all cases let \mathbf{u} be the unit vector at o tangent to λ_f pointing in the direction of $f(o)$, so that the counterclockwise angle from \mathbf{v} to \mathbf{u} is θ .

Assume $n = 1$, and suppose first that $t_1 = T$. Then the associated walk-with-jumps path consists of two segments: the first, of length st_1 , contained in γ_g —which by definition equals γ_1 —with one endpoint at o and \mathbf{v} pointing into it; the second, of length $j_1\ell$, sharing the other endpoint p_1 of the first and at a counterclockwise angle of θ from its outward-pointing tangent vector. The derivative of g_{t_1} at o takes \mathbf{v} to this outward-pointing vector, since g_{t_1} translates a distance of st_1 along γ_g , so it also takes \mathbf{u} to the vector pointing into the second segment at p . Therefore the second segment is contained in $g_{t_1}(\lambda_f) = \lambda_1$.

In this case $w = g_{t_1} f^{j_1} g_0$ in syllabic form (where g_0 is the identity). Note that $f^{j_1}(o)$ lies on λ_f at a distance of $j_1\ell$ from o in the direction of \mathbf{u} . Therefore g_{t_1} carries the segment of λ_f bounded by o and $f^{j_1}(o)$ to the second segment of the walk-with-jumps path, so $g_{t_1} f^{j_1}(o)$ is the path's endpoint. Similarly, the derivative

of f^{j_1} at o carries \mathbf{v} to a vector at $f^{j_1}(o)$ at a clockwise angle of θ from the outward-pointing unit vector to the segment of λ_f bounded by o and $f^{j_1}(o)$; it then follows from the chain rule that $w_*(\mathbf{v})$ is the walk's endvector.

Still taking $n = 1$, now suppose that $t_1 < T$. Then the associated walks-with-jumps path has three segments: the first two as in the previous case; and the third, of length $s(T - t_1)$, sharing the endpoint $q_1 \neq p_1$ of the second segment and at a *clockwise* angle of θ from its outward-pointing tangent vector. Thus by the previous case, the inward-pointing tangent vector to the third segment is $d(g_{t_1} f^{j_1})_o(\mathbf{v})$, and it follows that this segment lies in $\gamma_2 \doteq g_{t_1} f^{j_1}(\gamma_g)$. Moreover since $g_{T-t_1}(o)$ is the point on γ_g at distance $s(T - t_1)$ from o in the direction of \mathbf{v} , $(g_{t_1} f^{j_1})(g_{T-t_1}(o))$ is the far endpoint of the third walk segment from q_1 .

Since $w = g_{t_1} f^{j_1} g_{T-t_1}$ in this case, the above states exactly that $w(o)$ is the endpoint of the walk with jumps. And since $d(g_{T-t_1})_o(\mathbf{v})$ is the outward-pointing tangent vector at $g_{T-t_1}(o)$ to the sub-arc of γ_g bounded by o and $g_{T-t_1}(o)$, it follows from the chain rule as in the previous subcase that $w_*(\mathbf{v})$ is the endvector of the walk with jumps. This proves the Lemma's $n = 1$ case.

The $n > 1$ case is analogous, after applying the inductive hypothesis to the sub-walk with jumps having the same initial data, duration t_n , jump times (t_1, \dots, t_{n-1}) , and burst vector (j_1, \dots, j_{n-1}) . The product w_{2n-1} of the first $2n - 1$ syllables of w then plays the role of g_{t_1} in the $n = 1$ case above, as by the inductive hypothesis, $(w_{2n-1}(o), (w_{2n-1})_*(\mathbf{v}))$ is the endpoint-endvector pair of the sub-walk with jumps. That is, $w_{2n-1}(o)$ is the far endpoint from o of the walk-with-jumps path associated to the sub-walk—ie. the union of the first $2n - 1$ segments of the path associated to the walk specified in the Lemma—and $(w_{2n-1})_*(\mathbf{v})$ is the outward-pointing tangent vector to the $(2n - 1)^{\text{st}}$ segment. The two sub-cases now follow as in the $n = 1$ case, replacing j_1 there with j_n here and $T - t_1$ with $T - t_n$. \square

2.2. Perturbing jump times without changing the endpoint. We begin with a standard result that combines two assertions: that the isometry group of \mathbb{H}^2 acts transitively on it, and that an isometry is determined by where it sends a single point and tangent vector at that point. Below $UT\mathbb{H}^2$ is the unit tangent bundle of \mathbb{H}^2 , consisting of pairs (p, \mathbf{v}) for $p \in \mathbb{H}^2$ and \mathbf{v} a unit-length tangent vector at p , and $SL_2(\mathbb{R})$ is the group of 2×2 real matrices with determinant 1.

Proposition 2.8. *For a fixed $o \in \mathbb{H}^2$ and unit tangent vector \mathbf{v} at o , there is a diffeomorphism $PSL_2(\mathbb{R}) \rightarrow UT\mathbb{H}^2$ that sends $w \in PSL_2(\mathbb{R})$ to the pair $(w(o), w_*(\mathbf{v}))$ in $UT\mathbb{H}^2$, for $PSL_2(\mathbb{R}) = SL_2(\mathbb{R})/\{\pm I\}$.*

Proof. Taking \mathbb{H}^2 as the set of $z \in \mathbb{C}$ with positive imaginary part, $SL_2(\mathbb{R})$ acts on it via Möbius transformations: for $z \in \mathbb{H}^2$ and $a, b, c, d \in \mathbb{R}$ such that $ad - bc = 1$,

$$\begin{pmatrix} a & b \\ c & d \end{pmatrix} . z = \frac{az + b}{cz + d}.$$

This action extends to a smooth $SL_2(\mathbb{R})$ -action on the tangent bundle $\mathbb{H}^2 \times \mathbb{C}$ by taking $\begin{pmatrix} a & b \\ c & d \end{pmatrix}$ to act on the tangent vector $v \in \mathbb{C}$ at $z \in \mathbb{H}^2$ by multiplication by its derivative $1/(cz + d)^2$. This action preserves the hyperbolic Riemannian metric and hence restricts to an action on

$$UT\mathbb{H}^2 = \{(z, v) \in \mathbb{H}^2 \times \mathbb{C} \mid |v| = \Im z\}$$

It is an exercise to check that the $\mathrm{SL}_2(\mathbb{R})$ -action on \mathbb{H}^2 is transitive, and that the stabilizer of i is

$$\mathrm{SO}(2) = \left\{ \begin{pmatrix} \cos \theta & -\sin \theta \\ \sin \theta & \cos \theta \end{pmatrix} \right\}.$$

Such a matrix acts on a tangent vector v at i by multiplication by $1/(i \sin \theta + \cos \theta)^2 = e^{-2i\theta}$, ie. as rotation by -2θ . Therefore the extended action on $UT\mathbb{H}^2$ is also transitive, i.e., $UT\mathbb{H}^2$ is a *homogeneous space* of $\mathrm{SL}_2(\mathbb{R})$. Furthermore for any unit complex number v , regarded as a tangent vector to \mathbb{H}^2 at i , the stabilizer in $\mathrm{SL}_2(\mathbb{R})$ of (i, v) is the set

$$\left\{ \begin{pmatrix} \cos(n\pi) & -\sin(n\pi) \\ \sin(n\pi) & \cos(n\pi) \end{pmatrix} \right\} = \{\pm I\}.$$

Proposition 2.8 now follows directly from the characterization of homogeneous spaces, see eg. [11, Theorem 21.18]. This asserts that for a Lie group G acting on a homogeneous space X , and any fixed $x_0 \in X$, the smooth map $G \rightarrow X$ given by $g \mapsto g.x_0$ induces a diffeomorphism $G/H \rightarrow X$, where H is the stabilizer of x_0 in G . \square

Definition 2.9. For $T \in \mathbb{R}^+$ and $k \in \mathbb{N}$, let

$$T_k := \{(s_1, \dots, s_k) : 0 < s_1 < s_2 < s_3 < \dots < s_k < T\} \subset \mathbb{R}^k$$

and

$$\bar{T}_k := \{(s_1, \dots, s_k) : 0 \leq s_1 \leq s_2 \leq s_3 \leq \dots \leq s_k \leq T\} \subset \mathbb{R}^k.$$

Remark 2.10. \bar{T}_k is a simplex in \mathbb{R}^k which we view as encoding all possible walks with k jumps and duration T . A tuple $\mathbf{s} = (s_1, \dots, s_k)$ in \bar{T}_k encodes the same jump data as the pair $(t_1, \dots, t_n), (j_1, \dots, j_n)$ from Definition 1.1, where $n \leq k$ is the number of distinct s_i and for each $l \leq n$, t_l is a distinct such s_i , and j_l is the number of s_i equal to t_l .

T_k is the interior of \bar{T}_k , an open subset of \mathbb{R}^k consisting of paths that have burst vector $(1, 1, \dots, 1)$.

Lemma 2.11. Given the initial data $o, \mathbf{v}, s, \theta, \ell$ of a walk with jumps as in Definition 1.1, and $k \in \mathbb{N}, T > 0$: choose matrices representing the isometries f and $(g_t)_{t \in \mathbb{R}}$ of Lemma 2.1 so that f has positive trace and $g_0 = I$. Continuing to refer to these matrices as f and g_t , define $\Omega: \mathbb{R}^k \rightarrow \mathrm{SL}_2(\mathbb{R})$ by

$$\Omega(\mathbf{s}) = g_{s_1} f g_{s_2 - s_1} f \cdots g_{s_k - s_{k-1}} f g_{T - s_k},$$

for $\mathbf{s} = (s_1, \dots, s_k)$. This map is continuously differentiable.

Remark 2.12. If $\mathbf{s} \in \bar{T}_k$, for \bar{T}_k from Definition 2.9, then a computation shows that $\Omega(\mathbf{s}) \in \mathrm{SL}_2(\mathbb{R})$ represents the isometry w from Definition 2.6.

Proof. We will show that Ω has continuous partial derivatives, from which continuous differentiability will follow. To compute its i th partial derivative at $\mathbf{s} = (s_1, \dots, s_k) \in T_k$, we write $w \doteq \Omega(\mathbf{s})$ as $L_i f R_i$, for

$$(3) \quad L_i = g_{s_1} f g_{s_2 - s_1} \cdots f g_{s_i - s_{i-1}} \quad \text{and} \quad R_i = g_{s_{i+1} - s_i} f \cdots f g_{T - s_k}.$$

For small $t > 0$, we then have

$$\Omega(s_1, \dots, s_{i-1}, s_i + t, s_{i+1}, \dots, s_k) = L_i g_t f g_{-t} R_i$$

We may thus compute $\frac{\partial}{\partial s_i} \Omega(\mathbf{s}) = \frac{d}{dt} \Big|_{t=0} (D_i \circ C)(t)$ with the chain rule, where $D_i: \mathrm{SL}_2(\mathbb{R}) \rightarrow \mathrm{SL}_2(\mathbb{R})$ is given by $D_i(X) = L_i X R_i$ and $C(t) = g_t f g_{-t}$.

We compute $C'(0)$ using the “product rule for matrix multiplication”: for differentiable families (A_t) and (B_t) of 2×2 matrices,

$$\left. \frac{d}{dt} \right|_{t=0} (A_t B_t) = A_0 \left[\left. \frac{d}{dt} \right|_{t=0} B_t \right] + \left[\left. \frac{d}{dt} \right|_{t=0} A_t \right] B_0.$$

This yields $C'(0) = \mathfrak{g}f - f\mathfrak{g}$, where $\mathfrak{g} = \left. \frac{d}{dt} \right|_{t=0} g_t \in \mathfrak{sl}_2(\mathbb{R})$, since $g_0 = I$. Since the action of D_i on $\mathrm{SL}_2(\mathbb{R})$ restricts its action as a linear map of $M_2(\mathbb{R})$, the vector space of 2×2 matrices, D_i is its own derivative and we have

$$\frac{\partial}{\partial s_i} \Omega(\mathbf{s}) = L_i(\mathfrak{g}f - f\mathfrak{g})R_i.$$

The only \mathbf{s} -dependence above lies in the left- and right-multipliers L_i and R_i . These vary continuously with \mathbf{s} , by repeated applications of the continuity of the multiplication map on $\mathrm{SL}_2(\mathbb{R})$, and for the same reason so does $\partial\Omega/\partial s_i$. \square

Remark 2.13. *The partial derivatives computed above belong to the tangent space of $\mathrm{SL}_2(\mathbb{R})$ at w . Translating each back to the identity using left-multiplication by w^{-1} yields $R_i^{-1}f^{-1}(\mathfrak{g}f - f\mathfrak{g})R_i = R_i^{-1}(f^{-1}\mathfrak{g}f - \mathfrak{g})R_i$.*

$$f^{-1}(\mathfrak{g}f - f\mathfrak{g}) = 2s \sin \theta \sinh \ell \begin{pmatrix} -\cos \theta \sinh \ell & \cosh \ell + \sin \theta \sinh \ell \\ \cosh \ell + \sin \theta \sinh \ell & \cos \theta \sinh \ell \end{pmatrix}$$

Corollary 2.14. *For data $o, \mathbf{v}, s, \theta, \ell, k$ and T , the map $\psi_k: T_k \rightarrow UT\mathbb{H}^2$ given by composing the diffeomorphism from Proposition 2.8 with Ω from Lemma 2.11 is continuously differentiable.*

Remark 2.15. *The map ψ_k defined above takes a sequence of jump times $\mathbf{s} \in T_k$ to the endpoint-endvector pair of the walk with jumps determined by the prescribed initial data, \mathbf{s} , and duration T . In particular, the image of ψ_k is the collection of endpoints of all walks with k jumps, duration T , and initial data specified above.*

Proposition 2.16. *For $k > 3$ and $T_k \subset \mathbb{R}^k$ as in Definition 2.9, the map $\psi_k: T_k \rightarrow UT\mathbb{H}^2$ defined in Corollary 2.14 is not injective on any open subset $U \subseteq T_k$. That is: for any such U there exist distinct walks with jumps, sharing initial data and each with k jumps and duration T , each of whose sequence of jump times is contained in U , having the same endpoint-endvector pair.*

Proof. Since $UT\mathbb{H}^2$ is a 3-manifold we may assume that $\psi_k|_U$ maps to \mathbb{R}^3 , by replacing U with the smaller open set $U \cap \psi_k^{-1}(V)$ for a chart open set $V \subset UT\mathbb{H}^2$ intersecting $\psi_k(U)$, and post-composing with the chart map. If $\psi_k|_U$ were injective then by Brouwer’s Invariance of Domain Theorem, $\psi|_U$ would be a homeomorphism between U and $\psi(U) \subset \mathbb{R}^3$. However this contradicts the fact, a standard exercise in algebraic topology (cf. [7, Th. 2.26]), that no open subset of \mathbb{R}^k is homeomorphic to an open subset of \mathbb{R}^3 when $k > 3$. \square

Proposition 2.16 uses only the continuity of the map ψ_k to show that it is non-injective near every point of T_k , at arbitrarily small scales. Interpreted in terms of walks with jumps, this implies that for any given walk with at least three jumps, one can find distinct others which each differ from the original – hence also from each other – by an arbitrarily small perturbation of jump times, and have the same endpoint-endvector pair as each other (but not necessarily as the original walk with jumps). The next result gives a calculus tool for obtaining still finer information.

Proposition 2.17. *Fix $k \in \mathbb{N}$ at least 3, the initial data o , \mathbf{v} , $s > 0$, $\theta \in (0, \pi/2]$, $\ell > 0$ of a walk with jumps, and a duration $T > 0$, and let $T_k \subset \mathbb{R}^k$ be as in Definition 2.9. The set $U \subset T_k$ on which the derivative of the map $\psi_k: T_k \rightarrow UT\mathbb{H}^2$ from Corollary 2.14 has full rank is dense in T_k and open.*

Proof. Using the upper half-plane model we may assume without loss of generality that $o = i$ and $\mathbf{v} = (1, 0)$. In this case the isometries $(g_t)_{t \in \mathbb{R}}$ and f of Lemma 2.1 are represented by matrices

$$g_t = \begin{pmatrix} \cosh(st) & \sinh(st) \\ \sinh(st) & \cosh(st) \end{pmatrix} \text{ and } f = \begin{pmatrix} \cosh \ell + \sin \theta \sinh \ell & \cos \theta \sinh \ell \\ \cos \theta \sinh \ell & \cosh \ell - \sin \theta \sinh \ell \end{pmatrix}$$

Note that g_0 is the identity and f has positive trace, as required in Lemma 2.11. For $\mathfrak{g} = \left. \frac{d}{dt} \right|_{t=0} g_t \in \mathfrak{sl}_2(\mathbb{R})$, a computation now yields that $\mathfrak{g} = s \begin{pmatrix} 0 & 1 \\ 1 & 0 \end{pmatrix}$, and hence that

$$\mathbf{v} \doteq \mathfrak{g}f - f\mathfrak{g} = 2s \sin \theta \sinh \ell \begin{pmatrix} 0 & -1 \\ 1 & 0 \end{pmatrix}.$$

This matrix features in the description of $\frac{\partial}{\partial s_i} \Omega(\mathbf{s})$ in the proof of Lemma 2.11.

Claim 2.17.1. *For any $\mathbf{s} = (s_1, \dots, s_k) \in \overline{T}_k$, and any i , $\frac{\partial}{\partial s_i} \Omega(\mathbf{s}) \neq \mathbf{0}$.*

Proof of Claim. Appealing to Remark 2.13, we find that the claim holds if and only if $f^{-1}\mathbf{v} \neq \mathbf{0}$. This in turn can be easily verified using the descriptions of f and of \mathbf{v} recorded immediately above, together with the hypotheses on s , θ and ℓ implying that all scale factors of \mathbf{v} are positive. \square

Claim 2.17.2. *For any $\mathbf{s} = (s_1, \dots, s_k) \in \overline{T}_k$, and any $i < k$, $\frac{\partial}{\partial s_i} \Omega(\mathbf{s})$ and $\frac{\partial}{\partial s_{i+1}} \Omega(\mathbf{s})$ are linearly independent.*

Proof of claim. These two matrices are linearly *dependent* if and only if one is a scalar multiple of the other; ie, using the proof of Lemma 2.11, if and only if

$$k L_i \mathbf{v} R_i = L_{i+1} \mathbf{v} R_{i+1} \iff k \mathbf{v} (R_i R_{i+1}^{-1}) = (L_i^{-1} L_{i+1}) \mathbf{v}$$

for some $k \in \mathbb{R}$, where L_i and R_i are as described in (3). Using this description, the equality above is equivalent to the one below, defining $\delta_i = s_{i+1} - s_i$:

$$k \mathbf{v} (g_{\delta_i} f) = (g_{\delta_i} f) \mathbf{v}.$$

If we write $g_{\delta_i} f = \begin{pmatrix} a & b \\ c & d \end{pmatrix}$ then since \mathbf{v} is a scalar multiple of $\begin{pmatrix} 0 & -1 \\ 1 & 0 \end{pmatrix}$, the above equality is equivalent to following equations simultaneously holding:

$$-kc = b, \quad kd = a, \quad ka = d, \quad -kb = c.$$

Noting that we have $ad - bc = 1$, it follows that if the above all hold then $k = 1$, $a = d$, and $b = -c$. Performing the computations, we find that

$$a = d \iff \sin \theta \cosh(s\delta_i) \sinh \ell = 0$$

But this does not hold for $\theta \in (0, \pi)$ and $\ell > 0$, regardless of whether $\delta_i = 0$. \square

Claim 2.17.3. *For any fixed i , $1 < i < k$, there is an open dense set of $\mathbf{s} \in \overline{T}_k$ such that $\frac{\partial}{\partial s_{i-1}} \Omega(\mathbf{s})$, $\frac{\partial}{\partial s_i} \Omega(\mathbf{s})$, and $\frac{\partial}{\partial s_{i+1}} \Omega(\mathbf{s})$ are linearly independent.*

Proof of Claim. For arbitrary $\mathbf{s} = (s_1, \dots, s_k) \in \overline{T}_k$, taking L_i and R_i (and $L_{i\pm 1}$, $R_{i\pm 1}$) as in (3), the proof of Lemma 2.11 gives

$$\frac{\partial}{\partial s_{i-1}} \Omega(\mathbf{s}) = L_{i-1} \mathbf{v} R_{i-1}, \quad \frac{\partial}{\partial s_i} \Omega(\mathbf{s}) = L_i \mathbf{v} R_i, \quad \text{and} \quad \frac{\partial}{\partial s_{i+1}} \Omega(\mathbf{s}) = L_{i+1} \mathbf{v} R_{i+1}.$$

Multiplying the entire collection on the left by L_i^{-1} and on the right by R_i^{-1} , we find that the linear independence of this collection is equivalent to that of:

$$\mathcal{B}_0 \doteq \left\{ (L_i^{-1} L_{i-1}) \mathbf{v} R_{i-1} R_i^{-1}, \quad \mathbf{v}, \quad (L_i^{-1} L_{i+1}) \mathbf{v} (R_{i+1} R_i^{-1}) \right\}.$$

Taking $\delta_i = s_{i+1} - s_i$ and $\delta_{i-1} = s_i - s_{i-1}$, we further have:

$$L_{i-1}^{-1} L_i = g_{\delta_{i-1}} f = R_{i-1} R_i^{-1}, \quad \text{and} \quad L_i^{-1} L_{i+1} = g_{\delta_i} f = R_i R_{i+1}^{-1}.$$

Writing $g_{\delta_{i-1}} f$ as A_{i-1} and $g_{\delta_i} f$ as A_i , the collection in question has the form:

$$\mathcal{B}_0 = \left\{ A_{i-1}^{-1} \mathbf{v} A_{i-1}, \quad \mathbf{v}, \quad A_i \mathbf{v} A_i^{-1} \right\}$$

Taking $A_{i-1} = \begin{pmatrix} a & b \\ c & d \end{pmatrix}$ and $A_i = \begin{pmatrix} x & y \\ z & w \end{pmatrix}$, and dividing out the common scale factor $2s \sin \theta \sinh \ell > 0$ yields:

$$\mathcal{B} = \left\{ \begin{pmatrix} -ab - cd & -b^2 - d^2 \\ a^2 + c^2 & ab + cd \end{pmatrix}, \begin{pmatrix} 0 & -1 \\ 1 & 0 \end{pmatrix}, \begin{pmatrix} xz + yw & -x^2 - y^2 \\ z^2 + w^2 & -xz - yw \end{pmatrix} \right\}.$$

If there existed $\alpha, \beta, \gamma \in \mathbb{R}$ such that the linear combination

$$\alpha \begin{pmatrix} -ab - cd & -b^2 - d^2 \\ a^2 + c^2 & ab + cd \end{pmatrix} + \beta \begin{pmatrix} 0 & -1 \\ 1 & 0 \end{pmatrix} + \gamma \begin{pmatrix} xz + yw & -x^2 - y^2 \\ z^2 + w^2 & -xz - yw \end{pmatrix} = \begin{pmatrix} 0 & 0 \\ 0 & 0 \end{pmatrix},$$

then by considering upper-left entries we find that

$$\alpha(ab + cd) = \gamma(xz + yw),$$

and by considering lower-left and upper-right entries that

$$\alpha(a^2 + c^2) + \gamma(z^2 + w^2) = -\beta = \alpha(b^2 + d^2) + \gamma(x^2 + y^2).$$

Eliminating variables we thus find that either $\alpha = \beta = \gamma = 0$ or

$$(4) \quad \frac{xz + yw}{x^2 + y^2 - z^2 - w^2} = \frac{ab + cd}{a^2 - b^2 + c^2 - d^2}$$

The collection \mathcal{B} is thus linearly *dependent* if and only if equation (4) holds. Note that its left-hand side depends only on $\delta_i = s_{i+1} - s_i$, whereas the right depends only on $\delta_{i-1} = s_i - s_{i-1}$, among quantities that vary with \mathbf{s} . In particular, $\frac{\partial}{\partial s_{i+1}} a = \frac{\partial}{\partial s_{i+1}} b = \frac{\partial}{\partial s_{i+1}} c = \frac{\partial}{\partial s_{i+1}} d = 0$. We claim that the corresponding partial derivative of the left-hand side is positive.

This follows from direct computation. Taking $S_i = \sinh(s\delta_i)$ and $C_i = \cosh(s\delta_i)$, $S_\ell = \sinh \ell$ and $C_\ell = \cosh \ell$, and $s_\theta = \sin \theta$ and $c_\theta = \cos \theta$, we have:

$$A_i = \begin{pmatrix} x & y \\ z & w \end{pmatrix} = \begin{pmatrix} C_i C_\ell + s_\theta C_i S_\ell + c_\theta S_i S_\ell & S_i C_\ell - s_\theta S_i S_\ell + c_\theta C_i S_\ell \\ S_i C_\ell + s_\theta S_i S_\ell + c_\theta C_i S_\ell & C_i C_\ell - s_\theta C_i S_\ell + c_\theta S_i S_\ell \end{pmatrix}$$

Further computation now yields

$$\begin{aligned} xz + yw &= 2S_i C_i (S_\ell^2 + C_\ell^2) + 2c_\theta (S_i^2 + C_i^2) S_\ell C_\ell \\ &= \sinh(2s\delta_i) C_{2\ell} + c_\theta \cosh(2s\delta_i) S_{2\ell} \\ x^2 + y^2 - z^2 - w^2 &= 4s_\theta S_\ell C_\ell = 2s_\theta S_{2\ell}, \end{aligned}$$

where $C_{2\ell} = \cosh(2\ell)$ and $S_{2\ell} = \sinh(2\ell)$. The hypotheses $\theta \in (0, \pi/2]$ ensures that $c_\theta \geq 0$, and $S_i > 0$ since $\mathbf{s} \in T_k$. Thus using that $\delta_i = s_{i+1} - s_i$ and the

computation above, we find that $\frac{\partial}{\partial s_{i+1}}(xz + yw) > 0$. Again by the computation above, the denominator $x^2 + y^2 - z^2 - w^2$ of the left side of (4) does not depend on δ_i ; hence the left-hand side of (4) increases with s_{i+1} as claimed.

But this further implies Claim 2.17.3, since at any $\mathbf{s} = (s_1, \dots, s_k) \in T_k$ where equation (4) holds, increasing s_{i+1} while holding s_i and s_{i-1} constant produces points of T_k arbitrarily close to \mathbf{s} where (4) does not hold. Therefore the set of \mathbf{s} where $\frac{\partial}{\partial s_{i-1}}\Omega(\mathbf{s})$, $\frac{\partial}{\partial s_i}\Omega(\mathbf{s})$, and $\frac{\partial}{\partial s_{i+1}}\Omega(\mathbf{s})$ are linearly independent is dense. And it is also open, being the complement of the solution set to (4). \square

Given that U contains the open dense set described in Claim 2.17.3 for any fixed i , the claim immediately implies the result. \square

The next example shows that the set U of Proposition 2.17 where the derivative of ψ_k has full rank may be a proper subset of T_k .

Example 2.18. *Let us now consider a walk with jumps satisfying the hypotheses of Proposition 2.17, specialize to the case that $\theta = \pi/2$, and consider the equation (4) in this case. The computations below that equation specialize to:*

$$\begin{aligned} xz + yw &= \sinh(2s\delta_i) \cosh(2\ell) \\ x^2 + y^2 - z^2 - w^2 &= 2 \sinh(2\ell) \\ ab + cd &= \sinh(2s\delta_{i-1}) \\ a^2 - b^2 + c^2 - d^2 &= 2 \cosh(2s\delta_{i-1}) \sinh(2\ell) \end{aligned}$$

Setting the appropriate products equal to each other as in (4), and rearranging terms, we thus obtain the following equation:

$$\sinh(2s\delta_i) = \frac{\tanh(s\delta_{i-1})}{\cosh(2\ell)}.$$

This equation is satisfied if and only if $\frac{\partial}{\partial s_{i+1}}\Omega(\mathbf{s})$ lies in the span of $\frac{\partial}{\partial s_{i-1}}\Omega(\mathbf{s})$ and $\frac{\partial}{\partial s_i}\Omega(\mathbf{s})$.

We may regard it as recursively prescribing the value of δ_i , given δ_{i-1} . A given value of δ_1 therefore uniquely determines the set of values δ_i , $i > 1$, such that the span of all $\frac{\partial}{\partial s_i}\Omega(\mathbf{s})$ is two-dimensional.

Remark 2.19. *We could ask whether two walks with different durations can ever have the same endpoint. This may be less biologically relevant.*

We close this subsection by recording some consequences of the technical Proposition 2.17 for endpoints and endvectors of walks with jumps.

Corollary 2.20. *Fix $k \in \mathbb{N}$ greater than 3, the initial data o , \mathbf{v} , $s > 0$, $\theta \in (0, \pi/2]$, $\ell > 0$ of a walk with jumps, and a duration $T > 0$, and let $T_k \subset \mathbb{R}^k$ parametrize the set of walks with k jumps and the given initial data as in Definition 2.9. For any walk with jumps having the given initial data and duration, and whose sequence of jump times lies in the dense open set $U \subset T_k$ of Proposition 2.17, there exist arbitrarily small perturbations of its sequence of jump times yielding walks with jumps sharing its endpoint and endvector.*

Proof. Recall that U is defined to be the set of $\mathbf{s} \in T_k$ at which the derivative of the map $\psi_k: T_k \rightarrow UT\mathbb{H}^2$ from Corollary 2.14 has full rank, meaning rank three since $UT(\mathbb{H}^2)$ is three-dimensional. Since ψ_k is continuously differentiable, it is a

standard consequence of the Implicit Function Theorem that for any $\mathbf{s} \in U$, the level set of ψ_k containing \mathbf{s} intersects U in a submanifold of dimension $k - 3$. Recalling the interpretation of ψ_k from Remark 2.15, we see that the small perturbations of the present Corollary's statement lie on this submanifold, which has positive dimension since by hypothesis $k > 3$. \square

Corollary 2.21. *For any fixed $k \geq 3 \in \mathbb{N}$, initial data $o, \mathbf{v}, s > 0, \theta \in (0, \pi/2]$, $\ell > 0$ of a walk with jumps, and any duration $T > 0$, the set of endpoints of walks with jumps in \mathbb{H}^2 having the given initial data, k jumps, and duration T is the closure of its interior. In particular, it has non-empty interior.*

Proof. The set of endpoints of walks with jumps is the image of the simplex T_k of Definition 2.9 under the composition of the bundle projection $UT\mathbb{H}^2 \rightarrow \mathbb{H}^2$ with the map $\psi_k: T_k \rightarrow UT\mathbb{H}^2$ from Corollary 2.14. The bundle projection is a submersion, so by Proposition 2.17 this composition has full rank derivative at every point of the open dense subset $U \subset T_k$ identified there. As in the previous proof, the implicit function theorem now implies that for every $\mathbf{s} \in U$, there is an open neighborhood of $\psi_k(\mathbf{s})$ contained in $\psi_k(U) \subset \psi_k(T_k)$. Thus $\psi_k(U)$ is contained in the interior of the set of walk endpoints. Moreover, since U is dense in T_k , its image is dense in the set of endpoints. \square

Remark 2.22. *The diameter of the set of endpoints of walks with jumps having jump angle $\pi/2$ and other data identical to that of Corollary 2.21, meaning the supremum of the pairwise distances between these endpoints, can be explicitly bounded below along the lines of Proposition 1.10. A computation parallel to the proof of that result shows that the distance d between the endpoints of the walks with jumps corresponding to the vertices $(0, \dots, 0)$ and (T, \dots, T) of T_k satisfies:*

$$\cosh(d) - 1 = (\cosh(k\ell) - 1)(\cosh(sT) - 1)(\cosh(k\ell)\cosh(sT) - 1).$$

The diameter of the set of endpoints is thus bounded below by d , which can be seen to increase linearly with any of the individual quantities featured in its definition.

This exhibits a stark qualitative difference between the Euclidean and hyperbolic contexts: if one replaced " \mathbb{H}^2 " by " \mathbb{R}^2 " in its statement then the resulting set of endpoints would have diameter 0, being a single point.

Proposition 2.23. *Given the data $o, \mathbf{v}, s, \theta, \ell, T$, there exist two distinct sequences of jump times (t_1, \dots, t_n) and (t'_1, \dots, t'_n) that the corresponding walks with jumps have the same endpoints. In particular, the associated isometries $w = g_{t_1} f g_{t_2 - t_1} f \cdots g_{t_n - t_{n-1}} f g_{T - t_n}$ and $w' = g_{t'_1} f g_{t'_2 - t'_1} f \cdots g_{t'_n - t'_{n-1}} f g_{T - t'_n}$ are equal.*

Proof. By Proposition 2.16, the map ψ is not injective. Then $(w(o), w_*(\mathbf{v})) = (w'(o), w'_*(\mathbf{v}))$. By Proposition 2.8, $w = w'$. \square

Definition 2.24. A **semigroup** is a set together with an associative operation. A **free semigroup** is one that is isomorphic to the semigroup generated by a set with no relations.

Corollary 2.25. *Given the data, $o, \mathbf{v}, s, \theta, \ell, T$ the isometry f and the one parameter family g_t do not generate a free semigroup.*

3. MORE DIFFERENT WALKS WITH IDENTICAL ENDPOINTS

The previous section’s results, notably Corollary 2.20, show that there are distinct walks with the same duration and number of jumps, having identical endpoints. It is the nature of that approach to produce walks whose jump times are small perturbations of each other. In this section we will show by example that much more significant variation in jump times can still yield walks with jumps that have identical endpoints. We begin with Proposition 3.2, showing that a walk with a single, immediate jump can be well approximated for an arbitrary time by one in which a burst of two jumps occurs after a lag, followed by a regular sequence of jumps. We will then use a couple of tricks to turn a pair of such walks into a pair with identical durations and endpoints, in Proposition 3.5.

The family of examples produced here do not represent the full spectrum of possible ways in which walks with “significantly different” jump patterns may have identical endpoints; indeed, we do not feel that we have a firm handle on this issue at the moment. The construction we present makes non-generic choices at certain points for the sake of convenience. For instance, “two jumps” could easily be replaced by “ n jumps” in the paragraph above, for arbitrary $n \geq 2$. And we fix the jump angle at $\pi/2$ immediately below in order to take advantage of certain helpful hyperbolic trigonometric formulas for right-angled hyperbolic polygons.

In the lemma below, a *pentagon* is a concatenation of distinct geodesic arcs $\alpha_1, \dots, \alpha_5$ —its *sides*—such that α_i and α_{i+1} share an endpoint for each $i < 5$, as do α_1 and α_5 . Its *vertices* are $v_i \doteq \alpha_i \cap \alpha_{i+1}$, for $i < 5$, and $v_5 \doteq \alpha_5 \cap \alpha_1$. Its *angle* at v_i ($i = 1$ to $i = 4$) is measured counterclockwise from α_{i+1} to α_i , or for $i = 5$, from α_1 to α_5 . A pentagon is *self-intersecting* if non-adjacent sides intersect.

Lemma 3.1. *For any $\ell > 0$ there exist $0 < X_0 < X_1 \doteq \cosh^{-1}(\coth \ell \tanh(2\ell))$, such that for any $x \in (X_0, X_1)$ there is a self-intersecting pentagon $\alpha_1, \dots, \alpha_5$ satisfying the following conditions:*

- α_1 has length ℓ , α_2 length x , and α_3 length 2ℓ ;
- the angles at v_5, v_1, v_2 and v_3 all equal $\pi/2$; and
- α_3 intersects α_5 .

The angle δ at v_4 satisfies $\lim_{x \rightarrow X_0^+} \delta = 0$, and $\lim_{x \rightarrow X_1^-} \delta = \frac{\pi}{2} - \sin^{-1}\left(\frac{\cosh \ell}{\cosh(2\ell)}\right)$.

Proof. A quadrilateral in \mathbb{H}^2 with three right angles (called a “Lambert quadrilateral” in the classical geometry literature), is determined by the lengths of its two sides that have right angles at both of their vertices. If these two side lengths are ℓ and x then the final vertex angle $\gamma < \pi/2$ satisfies:

$$(5) \quad \cos \gamma = \sinh \ell \sinh x. \quad (\text{See [14, Thrm. 3.5.9].})$$

Note that this implies in particular that the product $\sinh \ell \sinh x$ can be at most 1. If this product is at least 1 then the two geodesics meeting the sides with lengths ℓ and x at right angles to their endpoints do not meet in \mathbb{H}^2 ; if it equals 1 then the two sides are “parallel”, ie. asymptotic, the quadrilateral has finite area, and we say it has a single “ideal vertex”.

If $\sinh \ell \sinh x < 1$ then applying [14, Thrm. 3.5.8] to the Lambert quadrilateral above gives the relation between ℓ , γ , and the length y of the side opposite the one with length ℓ recorded in the first equality below. Equation (5) then allows us to

replace $\sin \gamma$ in the denominator, yielding the second equality:

$$\cosh y = \frac{\cosh \ell}{\sin \gamma} = \frac{\cosh \ell}{\sqrt{1 - \sinh^2 x \sinh^2 \ell}}.$$

Note that if we fix ℓ and allow x to vary, this formula defines y as an *increasing* function of x . Setting $y = 2\ell$ and solving for x yields the formula for X_1 given in the Lemma's statement.

By the above, for any $x < X_1$, the following construction yields a geodesic arc α_3 crossing a geodesic ray β_5 that contains α_5 : Let α_1 and α_2 be arcs of lengths ℓ and x , respectively, meeting at right angles at a point v_1 ; let α_3 be a geodesic arc of length 2ℓ meeting α_2 at right angles at its endpoint v_2 opposite v_1 , so that α_1 and α_3 belong to the same half-space bounded by the geodesic containing α_2 ; and let β_5 be the geodesic ray meeting α_1 at right angles at its endpoint v_5 opposite v_1 , and contained in the same half-space bounded by the geodesic containing α_1 as α_3 .

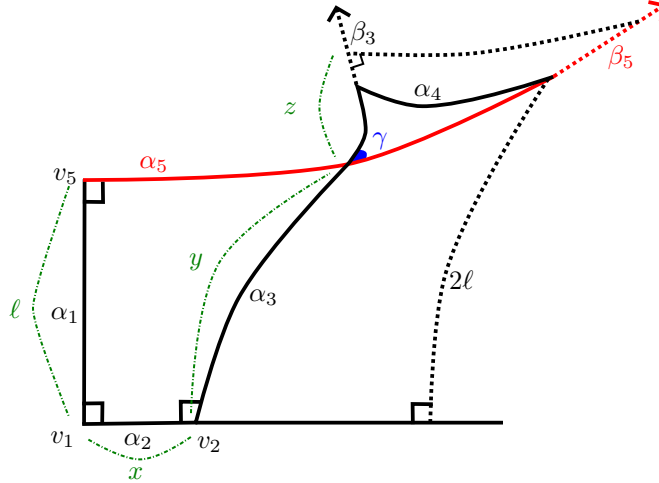


FIGURE 4. Accompanies the proof of Lemma 3.1.

Still taking $x < X_1$, for α_3 and β_5 as above, let $c = \alpha_3 \cap \beta_5$ and let β_3 be the geodesic ray with endpoint c , contained in the geodesic containing α_3 , in the opposite half-space bounded by the geodesic containing β_5 from α_2 . There exists a point on β_3 at a distance $z > 0$ from c such that a geodesic ray through this point, at right angles to β_3 in the half-space that β_5 points into, is parallel to β_5 . This point can be found because the geodesic through it forms a triangle, together with segments of β_3 and β_5 , that has one ideal vertex and angles of $\pi/2$ and γ (as defined in equation (5) above) at its other two angles. The distance z satisfies $\cosh z = 1/\sin \gamma$, see [14, Thm. 3.5.7]. Again fixing ℓ , and regarding γ and hence $z = z(\gamma)$ as functions of x , we find that since γ is a decreasing function of x , then z is an increasing function of x .

As $x \rightarrow 0^+$, $\gamma \rightarrow \pi/2$, $y \rightarrow \ell$, and $z \rightarrow 0$; as $x \rightarrow X_1$, $y \rightarrow 2\ell$. Thus $y + z$ is less than 2ℓ for x near 0 and greater than 2ℓ for x near X_1 . Since y and z each increase with x their sum does as well, so there is a unique $x = X_0$ with $0 < X_0 < X_1$ for

which $y + z = 2\ell$, and for all $x \in (X_0, X_1)$, $y < 2\ell < y + z$. By the equations above and the angle addition law for hyperbolic cosine, X_0 satisfies:

$$\cosh(2\ell) = \frac{\cosh \ell + \sinh \ell \sinh X_0 \cosh X_0}{1 - \sinh^2 X_0 \sinh^2 \ell}$$

Now given $x \in (X_0, X_1)$, let α_1 , α_2 , and α_3 be geodesic arcs as described above, with lengths ℓ , x , and 2ℓ , respectively; let $v_1 = \alpha_1 \cap \alpha_2$ and $v_2 = \alpha_2 \cap \alpha_3$; and let β_5 be the geodesic ray described above with its endpoint at the other endpoint v_5 of α_1 . Because $2\ell < y + z$, a geodesic ray from the other endpoint v_3 of α_3 , at right angles to α_3 and pointing into the same half-space bounded by the geodesic containing it as β_5 , does intersect β_5 . Let α_4 be the arc contained in this ray and joining v_3 to its point v_4 of intersection with β_5 . Finally, let α_5 be the arc of β_5 joining v_4 back to v_5 . This completes the construction of the self-intersecting pentagon. \square

Proposition 3.2. *For any initial data o , \mathbf{v} , s , θ , ℓ of a walk with jumps, such that the jump angle $\theta = \pi/2$, there exist $0 < X_0 < X_1$ (as defined above) such that for any $x \in (X_0, X_1)$ and $T_0 > 0$, there exist two walks with jumps sharing the given initial data and a common endpoint such that:*

- *the first has duration $T \geq T_0$ and a single jump at time 0; and*
- *the second has duration $T_1 < T$, its first jump (a burst of two) at time x/s , and a total number of jumps that increases linearly with T_0 .*

More precisely: there exists $K > 0$, depending only on x , such that $T \in [T_0, T_0 + K)$, and $b = b(x) > 0$ such that the second walk's jump times (t_1, t_2, \dots, t_n) satisfy $t_1 = x/s$, $t_2 < K$, and $t_i = t_2 + (i - 2)b$ for each $i \geq 2$.

Proof. For the value of ℓ in the given initial data, let $0 < X_0 < X_1$ be as in Lemma 3.1. Then for $x \in (X_0, X_1)$, arrange the pentagon given by that result so that its vertex v_1 is at o and \mathbf{v} points along the side α_2 of length x toward v_2 . Then the side α_1 of length ℓ is counterclockwise from α_2 at $v_1 = o$. As in the proof of Lemma 3.1, let β_5 be the ray sharing the other endpoint v_0 of α_1 and containing the pentagon's side α_5 . Since the first walk with jumps has a single jump at time 0, which has length ℓ , its sole nontrivial walk segment is contained in β_5 .

Since the second walk is prescribed to have a burst of two jumps at $t_1 = x/s$, its first walk segment is α_2 , its first jump segment is α_3 , and its second walk segment is contained in the geodesic ray β_4 that has an endpoint at v_3 and contains α_4 . We prescribe the second jump time t_2 to be larger than ℓ_4/s , where ℓ_4 is the length of α_4 —so the second walk segment contains α_4 —and with the property that the second jump axis is bisected by its intersection with β_5 . Precisely: taking $d_2 = st_2 - \ell_4$, we must have

$$(6) \quad \cosh d_2 = \frac{\sqrt{\sinh^2(\ell/2) + \sin^2 \delta}}{\cosh(\ell/2) \sin \delta},$$

where δ is the pentagon's angle at its vertex v_4 . This follows from the hyperbolic laws of sines and cosines; see Figure 5. There, the hyperbolic law of cosines gives that $\cosh h = \cosh d_2 \cosh(\ell/2)$, and the hyperbolic law of sines that $\sinh h = \sinh(\ell/2)/\sin \delta$. Substituting for h in the first equation yields the formula (6).

If we now prescribe for each $i > 2$ that $t_i - t_{i-1} = b \doteq 2d_2/s$, then the i th jump segment is also bisected by its intersection with β_5 for each such i . To see this, rotate

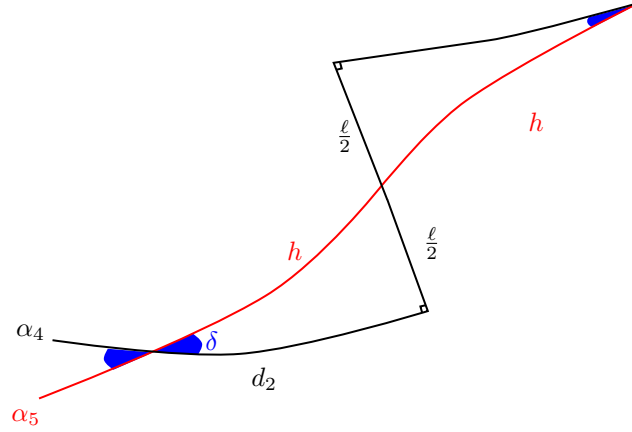


FIGURE 5. The triangle at the tip of the pentagon

the triangle of Figure 5 by 180 degrees about its vertex of intersection between the sides of length h and $\ell/2$: the resulting isometric copy also has its side of length h in β_5 , its side of length $\ell/2$ is the other half of the second walk's second jump segment, and its side of length d_2 is the first half of the third walk segment. Rotating this triangle 180° around its other non right-angled vertex yields the second half of the third walk segment and the first half of the third jump segment, and we proceed further by rotating around subsequent non right-angled vertices.

We now take $K = (\ell_5 + 2h)/s$, where ℓ_5 is the length of the pentagon's side α_5 and h is as in Figure 5. Then for any $T_0 > 0$, there is a walk with given initial data, a single jump at time 0, and duration in $[T_0, T_0 + K)$ that terminates at one of the intersection points of β_5 with a walk segment described in the paragraph above. These are segments of the second walk with jumps, which we run for as long as it takes to meet the first. \square

Note that the above construction of a specific pair of walks that have a common endpoint, has a biological interpretation: one way in which the endpoint can fail to faithfully encode the jump times is that a jump at time zero can be mimicked by a sequence of jumps at later times.

We now record an observation that will allow us to create “rotationally symmetric” walks with jumps.

Lemma 3.3. *For a walk with jumps with initial data $o, \mathbf{v}, s, \theta, \ell$, and duration T , if the jump times (t_1, \dots, t_{2n}) and burst vector (j_1, \dots, j_{2n}) are symmetric in the sense that $T/2 - t_i = t_{2n+1-i} - T/2$ and $j_i = j_{2n+1-i}$ for each $i \leq n$, then:*

- the associated walk with jumps path is itself symmetric under π -rotation around the walk's midpoint;
- denoting this rotation as ρ , the walk's endpoint and endvector are respectively $\rho(o)$ and $d\rho_o(-\mathbf{v})$; and
- the word w supplied by Lemma 2.7 that carries (o, \mathbf{v}) to the endpoint-endvector pair (p, \mathbf{w}) of the walk with jumps satisfies $\rho w \rho = w^{-1}$.

Proof. We call the i th walk segment (as in Definition 1.3) α_i , for $1 \leq i \leq 2n+1$, and the j th jump segment β_j for $1 \leq j \leq 2n$. Note that α_i has length $\ell_i = s\delta_i$ for $1 < i \leq 2n$, where $\delta_i = t_i - t_{i-1}$; and $\ell_1 = st_1$ and $\ell_{2n+1} = s(T - t_{2n})$. By hypothesis:

$$T/2 - t_1 = t_{2n} - T/2, \quad \Rightarrow \quad T - t_{2n} = t_1, \quad \Rightarrow \quad \ell_1 = \ell_{2n+1}.$$

Similarly, for $1 < i \leq n$, $\ell_i = \ell_{2n+2-i}$ since:

$$(7) \quad \begin{aligned} \delta_i &= [(T/2 - t_i) - (T/2 - t_{i-1})] \\ &= [(t_{2n+1-i} - T/2) - (t_{2n+1-(i-1)} - T/2)] = [t_{2n+2-i} - t_{2n+1-i}] = \delta_{2n+2-i}. \end{aligned}$$

The symmetry hypothesis on the jump vector similarly implies that β_j and β_{2n+1-j} have identical lengths for each j .

It follows from this that the midpoint of the associated walk with jumps path is the midpoint of α_{n+1} , so the rotation ρ by an angle π around this point takes α_{n+1} to itself. By construction of the walk with jumps, each of β_n and β_{n+1} intersects α_{n+1} at an angle of $\pi - \theta$ clockwise from the tangent vector pointing into α_{n+1} at their point of intersection. Since ρ exchanges the endpoints of α_{n+1} , and β_n and β_{n+1} have identical lengths, it also exchanges β_n and β_{n+1} . Now α_n and α_{n+2} respectively intersect β_n and β_{n+1} , each at an angle of $\pi - \theta$ counterclockwise from the tangent vector pointing into β_n or β_{n+1} , so ρ exchanges α_n with α_{n+2} since $\ell_n = \ell_{n+2}$.

Working our way outward from the midpoint as above, we ultimately find that ρ takes the entire walks with jumps path to itself. The assertion about the walk's endpoint and endvector now follow from this and Remark 1.4.

We now interpret the symmetry condition in terms of the word w supplied by Lemma 2.7 that carries (o, \mathbf{v}) to the endpoint-endvector pair (p, \mathbf{w}) of the walk with jumps. For this walk, w has the form

$$w = g_{t_1} f^{j_1} g_{\delta_2} f^{j_2} \dots g_{\delta_{2n}} f^{j_{2n}} g_{T-t_{2n}},$$

where for each $i > 1$, $\delta_i = t_i - t_{i-1}$ is the difference between successive jump times defined above. From (7) we have for each such i that $\delta_i = \delta_{2n+2-i}$. In particular, $\delta_{n+2} = \delta_n$, $\delta_{n+3} = \delta_{n-1}$, and so forth through $\delta_{2n} = \delta_2$. Also using that $T - t_{2n} = t_1$, we obtain the following visibly symmetric form for w :

$$w = (g_{t_1} f^{j_1} g_{\delta_2} \dots g_{\delta_n} f^{j_n}) g_{\delta_{n+1}} (f^{j_n} g_{\delta_n} \dots g_{\delta_2} f^{j_1} g_{t_1})$$

We now write $w = w_0 w_1$ where $w_0 = g_{t_1} f^{j_1} g_{s_2} \dots g_{s_n} f^{j_n} g_{s_{n+1}/2}$ is its "first half" and $w_1 = g_{s_{n+1}/2} f^{j_n} g_{s_n} \dots g_{s_2} f^{j_1} g_{t_1}$ its second. By Lemma 2.7, w_0 carries the origin o to the walk's midpoint. Therefore the rotation ρ by π about this point has the form $w_0 \rho_0 w_0^{-1}$, where ρ_0 is the π -rotation about o . Recalling that a π -rotation is its own inverse, we consider the conjugate of w by ρ :

$$\begin{aligned} \rho w \rho^{-1} &= (w_0 \rho_0 w_0^{-1}) w_0 w_1 (w_0 \rho_0 w_0^{-1}) \\ &= w_0 \rho_0 w_1 w_0 \rho_0 w_0^{-1} = w_0 (\rho_0 w_1 \rho_0) (\rho_0 w_0 \rho_0) w_0^{-1} \end{aligned}$$

We claim now that $\rho_0 w_i \rho_0 = w_{1-i}^{-1}$ for $i = 0$ and 1 , from which it will follow that $\rho w \rho = w^{-1}$ using the above. This uses the fact that ρ_0 conjugates f to f^{-1} , and likewise g_t for any $t \in \mathbb{R}$, since their axes run through its fixed point o . (One can

check this fact directly by taking $o = \mathbf{0}$ and $\mathbf{v} = \mathbf{e}_1$ in the Poincaré disk model and using the explicit descriptions below.)

$$\rho_0 = \begin{pmatrix} i & 0 \\ 0 & -i \end{pmatrix} \quad \text{and} \quad g_t = \begin{pmatrix} \cosh(t/2) & \sinh(t/2) \\ \sinh(t/2) & \cosh(t/2) \end{pmatrix}$$

Now inserting $\rho_0 \rho_0$, a form of the identity, between each syllable of w_0 for instance, we obtain:

$$\begin{aligned} \rho_0 w_0 \rho_0 &= (\rho_0 g_{t_1} \rho_0) (\rho_0 f^{j_1} \rho_0) (\rho_0 g_{s_2} \rho_0) \cdots (\rho_0 g_{s_{n+1}/2} \rho_0) \\ &= g_{t_1}^{-1} f^{-j_1} g_{s_2}^{-1} \cdots g_{s_{n+1}/2}^{-1} = w_1^{-1} \end{aligned}$$

Likewise for w_1 , and the claim, and hence the lemma, holds. \square

We now exploit Lemma 3.3 to promote Proposition 3.2's walks with jumps to a pair sharing an endpoint *and* endvector.

Proposition 3.4. *For any initial data $o, \mathbf{v}, s, \theta, \ell$ of a walk with jumps, such that the jump angle $\theta = \pi/2$, there exist $b, K > 0$ and $0 < X_0 < X_1$ such that for any $T_0 > 0$ and $x \in (X_0, X_1)$, there exist two walks with jumps sharing the given initial data and a common endpoint and endvector:*

- *The first has duration $T_2 \in [2T_0, 2T_0 + 2K)$ and two jumps, at time 0 and $t = T_2$, with burst vector $(1, 1)$;*
- *The second has jump times (t_1, \dots, t_{2n}) and burst vector $(2, 1, \dots, 1, 2)$ for some $n \geq 2$, where $t_1 = x/s$, $t_{2n} = 2T_1 - t_1$ and for $2 \leq i \leq n$, $t_i = t_2 + (i - 2)b$ and $t_{2n+1-i} = 2T_1 - t_i$, where $2T_1$ is its duration.*

Proof. For the given initial data, let $0 < X_0 < X_1$ be supplied by Proposition 3.2. Then for $T_0 > 0$ and $x \in (X_0, X_1)$ let that result supply a duration T for a first walk and jump times (t_1, t_2, \dots, t_n) for a second, with burst vector $(2, 1, \dots, 1)$ such that the two walks with jumps share an endpoint. Let T_1 be the duration of the second walk with jumps supplied by Proposition 3.2.

We construct the walks with jumps for the current result to be rotationally symmetric in the sense of Lemma 3.3, with those supplied by Proposition 3.2 as initial segments (up to their midpoints). Thus we take the first to have duration $T_2 \doteq 2T$ and single jumps at times 0 and $T_2 = T_2 - 0$; and the second to have duration $2T_1$ and jump times and burst vector as given in the statement. This walk's jump data is thus symmetric, i.e., the jump times satisfy the equation $T_1 - t_i = t_{2n+1-i} - T_1$ for each i , and the burst vector entries also match, so by Lemma 3.3 its associated walk-with-jumps path is symmetric by the rotation ρ about its midpoint.

The first walk with jumps also has symmetric jump data, so its walk-with-jumps path is also rotationally symmetric. But these two paths have the same midpoint, since by construction their initial segments are the walks with jumps given by Proposition 3.2 and these have a common endpoint. Hence the current walks with jumps have both a common endpoint $\rho(o)$ and endvector $d\rho_o(-\mathbf{v})$. \square

The walks constructed in Proposition 3.4 have different durations and numbers of jumps, but this can be fixed by reversing their roles and doubling again.

Proposition 3.5. *For any initial data $o, \mathbf{v}, s, \theta, \ell$ of a walk with jumps, such that the jump angle $\theta = \pi/2$, there exist $b, K > 0$ and $0 < X_0 < X_1$ such that for any $T_0 > 0$ and $x \in (X_0, X_1)$, there exist two walks with jumps having the given initial data and identical durations $T_2 + 2T_1$ —for $T_2 \in [2T_0, 2T_0 + 2K)$ and some $T_1 > 0$ —numbers of jumps, and endpoint and endvector:*

- The first has jump times $(0, T_2, T_2 + t_1, \dots, T_2 + t_{2n})$, for some $n \geq 2$, and burst vector $(1, 1, 2, 1, \dots, 1, 2)$;
- The second has jump times $(t_1, \dots, t_{2n}, 2T_1, 2T_1 + T_2)$, for the same n , and burst vector $(2, 1, \dots, 1, 2, 1, 1)$.

In each case above, $t_1 = x/s$, $t_{2n} = 2T_1 - t_1$ and for $2 \leq i \leq n$, $t_i = t_2 + (i - 2)b$ and $t_{2n+1-i} = 2T_1 - t_i$.

Proof. To construct the first and second walks here we use the corresponding walks from Proposition 3.4 as their initial segments, so that result supplies T_2 , T_1 , and the jump times t_1, \dots, t_n . The initial segments thus have the same endpoint and endvector, after a duration of T_2 for the first and $2T_1$ for the second. For the terminal segment of the first walk here, we then use a copy of the *second* walk supplied by Proposition 3.4; and conversely, for the terminal segment of the second walk we use a copy of the previous Proposition's *first* walk. \square

4. CONSEQUENCES OF NEGATIVE CURVATURE LEADING TO DISTINCT ENDPOINTS

In this section, a counterpoint to the previous one, we show that both the pattern and number of jumps can affect the endpoint of a walk with jumps. First, in Section 4.1, we give a criterion for producing walks with identical initial data, duration, and number of jumps but different endpoints. We subsequently prove quasigeodesicity of walk-with-jumps paths, in Section 4.2, a result that has as a particular consequence that having a different enough number of jumps leads to different endpoints.

4.1. Future quadrants and points of no return.

Lemma 4.1. *For a walk with jumps with the data of Lemma 2.7, the distinct walk axes of Definition 2.6 are pairwise disjoint. Furthermore if $j < i < k$, then γ_j and γ_k lie in distinct components of $\mathbb{H}^2 \setminus \gamma_i$. For each i , the shortest distance d from γ_i to γ_{i+1} satisfies $\sinh(d/2) = \sin \theta \sinh(\ell/2)$.*

The distinct jump axes are also pairwise disjoint and satisfy the analogous separation property; and for $i > 1$, the shortest distance x_i from λ_{i-1} to λ_i satisfies $\sinh(x_i/2) = \sin \theta \sinh(s(t_i - t_{i-1})/2)$.

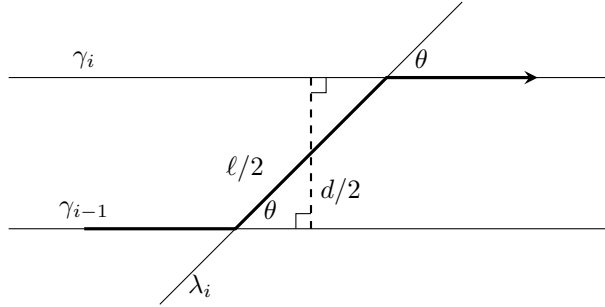


FIGURE 6. Two walk axes γ_{i-1} and γ_i , and a jump axis λ_i , with a segment of a walk-with-jumps path in bold. The shortest distance between walk axes is along the dashed arc.

Proof. We can take the γ_i and λ_j to be oriented “in the direction of travel” (i.e., in the direction that the relevant conjugate of the g_t or f translates). For a fixed $i > 0$, γ_{i-1} and γ_i both intersect λ_i . At each intersection, the angle from its positive direction to that of λ is equal to θ . If γ_i and γ_{i-1} had a point of intersection they would thus form a triangle, together with λ_i , whose angles at the edge contained in λ_i were θ and $\pi - \theta$. This would contradict that the angle sum of a hyperbolic triangle with at least one compact vertex is less than π .

The same argument also rules out γ_i and γ_{i-1} sharing an ideal endpoint, so they are at a nonzero distance from each other. The minimum distance d is attained at endpoints of a unique geodesic arc that meets each of γ_{i-1} and γ_i at right angles.

To determine d , we first note that the π -rotation around the midpoint of the arc of λ_i that joins γ_{i-1} to γ_i takes λ_i to itself and exchanges γ_{i-1} with γ_i . (This can be seen from the fact that it interchanges their tangent vectors at their points of intersection with λ_i , which determine the geodesics.) The geodesic arc joining γ_{i-1} to γ_i is therefore also preserved by this rotation, so it contains its fixed point as a bisector.

The formula for d now follows from the hyperbolic law of sines, see Figure 6. The distance x_i between λ_{i-1} and λ_i is established analogously, since these geodesics are joined by an arc of γ_i of length $s(t_i - t_{i-1})$. (The main difference from the previous case being that this depends on i , since the time intervals between jumps can vary)

We finally note that by construction of the walk with jumps, the segment of λ_i joining γ_{i-1} to γ_i is on the opposite side of γ_i from the arc of λ_{i+1} joining γ_i to γ_{i+1} (for $0 < i < n$). From this, it follows that γ_i separates γ_{i-1} from γ_{i+1} . A quick inductive argument now ensures for all $j < i < k$ that γ_j and γ_k lie in opposite complementary components of γ_i . \square

Corollary 4.2. *For a walk with jumps with the data of Lemma 2.7, the parametrization of the associated walk-with-jumps path given in Definition 1.3 defines an embedding of the parameter interval to \mathbb{H}^2 .*

For each $i \geq 1$, any points a , p_i , and b on the walk-with-jumps path such that the parameter value of a (respectively, b) is less (resp. greater) than that of p_i determine a triangle in \mathbb{H}^2 whose interior angle at p_i is at least $\pi - \theta$. The same angle bound likewise holds for an analogous triangle with vertices at a , q_i , and b .

Proof. Since the parametrization given in Definition 1.3 is by arclength on any sub-interval of the parameter interval that maps to a walk or jump segment, it is injective on such sub-intervals. Moreover, walk and jump segments that share an endpoint do not intersect outside this endpoint, since it is a general property of hyperbolic geodesics that they intersect in at most a single point. Therefore for parameter values t and $t' \neq t$ mapping to the same point, we may assume that they do not belong to the same or adjacent sub-intervals as above. However then the walk or jump segments that they map to, which are not identical and do not share an endpoint, are separated by the walk or jump axis containing any segment that lies between these two on the walk-with-jumps path, by Lemma 4.1.

We address the triangle Δ with vertices at a , p_i , and b ; the other case is similar. By Lemma 2.7, a lies on γ_1 , p_i on $\gamma_i \cap \lambda_i$, and q_i on $\lambda_i \cap \gamma_{i+1}$. Thus by Lemma 4.1, the edge of Δ joining a to p_i lies entirely in the half-plane bounded by γ_i that does not contain q_i and the half-plane bounded by λ_i that does not contain p_{i+1} .

These half-planes have angle of intersection θ at p_i , so the interior angle of T here exceeds the complementary angle $\pi - \theta$, see Figure 7. \square

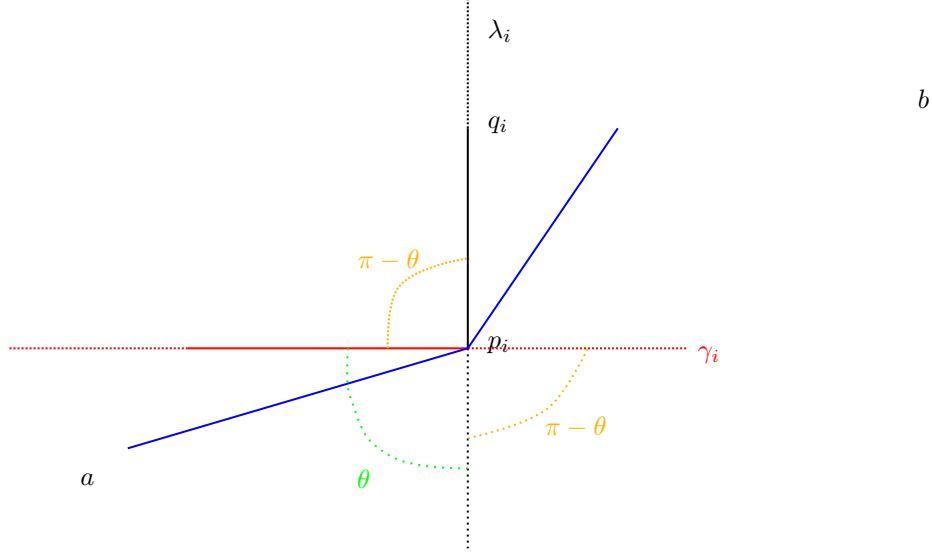


FIGURE 7. To accompany Corollary 4.2

We begin by formally defining a notion that has appeared already in the proof of Lemma 2.7.

Definition 4.3. Suppose a walk with jumps is specified by initial data $o, \mathbf{v}, s, \theta, \ell$; duration T ; jump time sequence (t_1, \dots, t_n) ; and burst vector (j_1, \dots, j_n) . For any $T_0 \leq T$, the *duration- T_0 initial segment* of the given walk with jumps is the one sharing the same initial data; with duration T_0 ; sequence of jump times (t_1, \dots, t_k) , where $k \leq n$ is the largest index such that $t_k \leq T_0$; and burst vector (j_1, \dots, j_k) for the same k . Conversely, we say that the original walk with jumps is obtained by *prolonging* any initial segment.

Remark 4.4. Let $w \in \mathrm{PSL}_2(\mathbb{R})$ be the word in syllable form with respect to some $f, g_t \in \mathrm{PSL}_2(\mathbb{R})$ associated to a walk with jumps by Lemma 2.7. For any initial segment of the given walk with jumps, the syllable form of its associated word $w_0 \in \mathrm{PSL}_2(\mathbb{R})$ is a prefix of w . Specifically, $w = w_0 w_1$ for some w_1 , where the syllable form of w can be determined from the syllable forms of w_0 and w_1 by replacing the last syllable g_{s_0} of w_0 and the first syllable g_{s_1} of w_1 with a single syllable $g_{s_0+s_1}$.

The result below is another consequence of Lemma 4.1. Given a bi-infinite geodesic $\gamma \subset \mathbb{H}^2$ such as one of the walk or jump axes of a walk with jumps, a *half-plane bounded by γ* is the closure of one component of $\mathbb{H}^2 - \gamma$. Its *complementary half-plane* is the closure of the other component.

Corollary 4.5. Suppose a walk with jumps is specified by initial data $o, \mathbf{v}, s, \theta, \ell$; duration T ; jump time sequence (t_1, \dots, t_n) , $n \geq 1$; and burst vector (j_1, \dots, j_n) . Let γ_g and λ_f be as in Lemma 2.1, and let γ_i , for $i \in \{1, \dots, n+1\}$, and λ_j , for $j \in \{1, \dots, n\}$, be the walk and jump axes from Definition 2.6. Then:

- Let H_0^+ be the half-plane bounded by $\gamma_g = \gamma_1$ that contains γ_2 and K_0^+ the half-plane bounded by λ_f that contains λ_1 . Then $H_0^+ \cap K_0^+$ contains the entire associated walks-with-jumps path.
- For each $i \in \{1, \dots, n\}$ let H_i^- be the half-plane bounded by γ_{i+1} that contains o and K_i^- the half-plane bounded by λ_i that contains o . The entire walks-with-jumps path of the duration- t_i initial segment is contained in $H_i^- \cap K_i^-$, and the remainder of the full walk-with-jumps path is contained in the intersection of the complementary half-planes $H_i^+ \cap K_i^+$.

Moreover, taking λ_{n+1} to be the geodesic through the endpoint of the walk with jumps at an angle of θ to γ_{n+1} , measured counterclockwise from the endvector, there is a half-plane K_{n+1}^- bounded by λ_{n+1} such that $H_n^- \cap K_{n+1}^-$ contains the entire walk-with-jumps path.

Proof. We claim that H_0^+ contains each axis γ_i for $i \geq 1$. Of course H_0^+ contains its boundary γ_1 , and the case $i = 2$ holds by definition. Now for $i \geq 2$, supposing that $\gamma_j \subset H_0^+$ for each $j \leq i$, we claim that γ_{i+1} is also contained in H_0^+ . This follows from Lemma 4.1, which asserts that γ_i separates γ_{i+1} from γ_{i-1} , so since γ_{i-1} and γ_i lie in H_0^+ , so does γ_{i+1} . The claim thus follows by induction.

By Lemma 2.7, it now follows that H_0^+ contains each walk segment of the associated walk-with-jumps-path. And since each jump segment is a geodesic arc joining endpoints of two walk segments, and H_0^+ is convex, it also contains each jump segment. Therefore H_0^+ contains the entire associated walk-with-jumps path. An entirely analogous argument shows that K_0^+ does as well, and the first bulleted claim is proved.

We now prove the second claim. We claim that if $j \leq i + 1$, then γ_j is in H_i^- , the half plane bounded by γ_{i+1} that contains o . Indeed, if $j = i + 1$ the result is clear, so we assume $j < i + 1$. In the special case, $j = 0$, Lemma 4.1 implies γ_0 is contained in a distinct half plane bounded by γ_0 and γ_0 contains o . For $0 < j < i + 1$, Lemma 4.1 implies that γ_j separates $o \in \gamma_0$ from γ_j . Therefore, the half plane bounded by γ_{i+1} that contains γ_j must be the one that contains o .

If x lies in the duration- t_i initial segment, then x either lies on one of the γ_j for $j < i + 1$ or lies on a geodesic between $\gamma_{j_1}, \gamma_{j_2}$ where $j_1, j_2 \leq i + 1$. In the first case, we immediately have that x lies in H_i^- , and in the second x lies in H_i^- by convexity of half planes. A similar argument shows that x also lies in K_i^- . Then $x \in H_i^- \cap K_i^-$.

On the other hand, if y lies in the remainder of the full walk-with-jumps path, then y lies on some γ_j for $j \geq i + 1$ or y lies on a geodesic between $\gamma_{j_1}, \gamma_{j_2}$ where $j_1, j_2 \geq i + 1$. Lemma 4.1 implies that if $j > i + 1$, then γ_{i+1} separates γ_j from γ_0 which contains o . Therefore, for $j \geq i + 1$, γ_j lies in H_i^+ , the half plane bounded by γ_{i+1} that does not contain o . Therefore, $y \in H_i^+$ by convexity of H_i^+ . A similar argument shows y also lies in K_i^+ . Therefore, $y \in H_i^+ \cap K_i^+$.

We now address the Corollary's final claim. Note that each of λ_{n+1} and λ_n intersect γ_{n+1} at an angle of θ : the former by construction, and the latter as observed in Lemma 4.1. They coincide if $t_n = T$; otherwise they do not intersect (also as observed in Lemma 4.1). In the former case, take $K_{n+1}^- = K_n^-$. In the latter, let K_{n+1}^- be the half-plane bounded by λ_{n+1} and containing λ_n . Then K_{n+1}^- contains the $(n + 1)$ st walk segment, since the endpoints of this segment lie on λ_{n+1}

and λ_n , and it contains the half-plane K_n^- opposite this segment. Therefore by the previous claim, K_{n+1}^- contains the entire walk-with-jumps path. \square

Definition 4.6. Motivated by the second bullet of Corollary 4.5, for H_n^+ , λ_{n+1} , and K_{n+1}^- as defined there, we call K_{n+1}^+ the half-plane bounded by λ_{n+1} opposite K_{n+1}^- and deem the intersection $H_n^+ \cap K_{n+1}^+$ of half-planes the *future quadrant* of the walk with jumps specified there.

4.2. Quasigeodesicity. In this section we will show that the walk-with-jumps paths in \mathbb{H}^2 from Definition 1.3 are “quasi-geodesic”. This property is well known to have important consequences in the study of negatively curved spaces. A key consequence for our application, recorded in Corollary 4.13 below, is that walks with different (enough) *numbers* of jumps have different endpoints, irrespective of any other consideration. As in the previous subsection, our results here are *effective*, meaning that we produce explicit constants.

Definition 4.7. For a fixed $\lambda \in (0, 1]$ and $\epsilon \geq 0$, a (λ, ϵ) -*quasi-geodesic* in a metric space (X, d) is a map $c : I \rightarrow X$, where $I \subset \mathbb{R}$ is an interval, such that for all $t, t' \in I$:

$$\lambda|t - t'| - \epsilon \leq d(c(t), c(t')) \leq \frac{1}{\lambda}|t - t'| + \epsilon.$$

This definition asserts that the path c does not shrink or expand distance by more than a multiplicative factor of λ and an additive factor of ϵ . In applying the notion to a walk-with-jumps path we will leverage the fact that it is a broken geodesic. Our parametrization described in Definition 1.3 is by arclength on each piece, so the right-hand inequality above will automatically hold for any $\lambda \in (0, 1]$ and $\epsilon \geq 0$.

Proposition 4.8 (Hyperbolic Law of Cosines, [2, I.2.7]). *Let Δ be a hyperbolic triangle with vertices A, B, C . Let $a = d(B, C)$, $b = d(C, A)$, and $c = d(A, B)$. Let θ denote the vertex angle at C . Then*

$$\cosh c = \cosh a \cosh b - \sinh a \sinh b \cos \theta$$

In particular, if $|\theta| = \frac{\pi}{2}$, then:

$$\cosh c = \cosh a \cosh b$$

Lemma 4.9. *For a triangle $\Delta \subset \mathbb{H}^2$ with vertices A, B , and C and opposite side lengths a, b , and c respectively, if Δ has interior angle θ at C then*

$$a + b - c < \delta_\theta \doteq \ln \left(\frac{2}{1 - \cos \theta} \right).$$

This bound is sharp, not attained, but asymptotically approached as $a = b \rightarrow \infty$.

Remark 4.10. *We fix $\theta = \pi/2$ to illustrate the strong contrast between \mathbb{R}^2 and \mathbb{H}^2 . By the result above, for a right triangle in \mathbb{H}^2 with hypotenuse of length c , the difference $a + b - c$ is universally bounded above by $\ln 2$. On the other hand, for an isosceles right triangle in \mathbb{R}^2 with shorter side length $a = b$ the difference $a + b - c = (2 - \sqrt{2})a$ increases linearly with a .*

Proof. Using the hyperbolic law of cosines from Proposition 4.8, we consider $a + b - c$ as a function $f_\theta(a, b)$ on the quadrant $\{a, b \geq 0\}$ in the ab -plane by substituting

$$c = \cosh^{-1}(\cosh a \cosh b - \sinh a \sinh b \cos \theta).$$

A somewhat messy calculus computation gives that the gradient vector $\nabla f_\theta(a, b)$ is a positive scalar multiple of $(\sinh^2 B, \sinh^2 A)$. Thus at any $(a, b) \neq (0, 0)$ (the global minimum of f_θ), the gradient points away from the origin and toward the diagonal (x, x) . So for instance, for any fixed $X > 0$, the maximum of f_θ on $[0, X]^2$ occurs at (X, X) . Moreover, $f_\theta(x, x)$ is an increasing function of x , and it follows that the values of f_θ on the entire quadrant are bounded above by $\delta_\theta = \lim_{x \rightarrow \infty} f_\theta(x, x)$.

To evaluate the limit, we exponentiate $f_\theta(x, x)$ and use the fact that $\cosh^{-1} y = \ln(y + \sqrt{y^2 - 1})$ to write

$$e^{f_\theta(x, x)} = \frac{e^{2x}}{\cosh^2 x - \sinh^2 x \cos \theta + \sqrt{(\cosh^2 x - \sinh^2 x \cos \theta)^2 - 1}}$$

Multiplying top and bottom by e^{-2x} then evaluating the limit and taking a natural log yields the formula for δ_θ given above. \square

Proposition 4.11. *For a walk with jumps with initial data $o, \mathbf{v}, s, \ell, \theta$; of duration T and with jump times (t_1, \dots, t_n) and burst vector (j_1, \dots, j_n) , the distance d from o to the walk's endpoint satisfies*

$$sT + \ell N \geq d \geq sT + \ell N - 2n\delta_{\pi-\theta},$$

for δ_θ as in Lemma 4.9, where $N = \sum_{i=1}^n j_i$ is the number of jumps. Moreover, supposing that $\delta_{\pi-\theta} < \ell/2$, define

$$(8) \quad \lambda = \frac{\ell - 2\delta_{\pi-\theta}}{\ell}.$$

Then the associated walk-with-jumps path is a $(\lambda, 2\delta_{\pi-\theta})$ -quasi-geodesic.

Remark 4.12. *The length lower bound above implies that “more bursty” walks are closer to geodesic. To support this assertion, note that $n \leq N$ since N is the total number of jumps whereas n is the number of jump times. Thus it is reasonable to take $N - n$ to measure the “burstiness” of the walk: for a fixed N , the growth of $N - n$ corresponds to the same number of jumps being concentrated at fewer times. As Proposition 4.11's lower bound decreases with n , it also increases with $N - n$.*

Proof. The upper bound on the distance between endpoints follows from the fact that the walk-with-jumps path of Definition 1.3 is a broken geodesic joining o to the walk's endpoint, of total length $sT + \ell \cdot \sum_i j_i$. This also implies that the distance between any two points on the path is bounded above by their distance *along* the path, ie. the difference between their parameter values if it is parametrized piecewise by arclength as in the Definition. This implies the upper bound needed for quasigeodesicity in Definition 4.7.

To prove the Proposition's lower bound on the distance between endpoints we sequentially apply Lemma 4.9 and Corollary 4.2, first to the triangle with vertices o, p_i , and q_i then to the triangle with vertices o, q_i , and p_{i+1} , for i increasing from 1 to n . (For $i = n$ we interpret “ p_{i+1} ” to refer to the walk's endpoint.) From these we obtain inductively that for each i , the distance from o to q_i is at least $st_i + \ell \cdot \sum_{k=1}^i j_k - (2i-1)\delta_{\pi-\theta}$, and from o to p_{i+1} , at least $st_{i+1} + \ell \cdot \sum_{k=1}^i j_k - 2i\delta_{\pi-\theta}$ (where for $i = n$ we interpret “ t_{i+1} ” as T).

For arbitrary x and y on the walk-with-jumps path, an entirely analogous argument shows that the distance from x to y is at least $d_0 - k\delta_{\pi-\theta}$, where d_0 is the

length of the sub-path bounded by x and y and k is the number of p_i and q_i that lie within this sub-path. The sub-path bounded by x and y contains least $\frac{k-2}{2}$ jump segments, with the lower bound attained only if x and y each lie in separate jump segments. Thus using that $d_0 > \frac{k-2}{2}\ell$, we have

$$d(x, y) \geq d_0 - \frac{k-2}{2}(2\delta_{\pi-\theta}) - 2\delta_{\pi-\theta} \geq d_0 \left(1 - \frac{2\delta_{\pi-\theta}}{\ell}\right) - 2\delta_{\pi-\theta}.$$

The right-hand quantity in parentheses above is exactly λ from (8), so we have proved the needed lower bound for quasigeodesicity. \square

Corollary 4.13. *Let $o, \mathbf{v}, s, \ell, \theta$ be the initial data of a walk with jumps. Supposing that $\delta_{\pi-\theta} < \ell/2$, for δ as in Lemma 4.9, define λ as in (8). Then for any natural numbers M and N with $M < \lambda N$, and any fixed $T > 0$, no two walks with jumps that share the initial data above and duration T have the same endpoint if the first has M jumps and the second, N .*

The Corollary follows directly by comparing Proposition 4.11's upper bound for the walk with M jumps to the lower bound for the walk with N jumps, and applying the fact that $M < \lambda N$ and $n \leq N$ to show that the endpoint of the walk with M jumps is closer to o than the endpoint of the walk with N jumps.

As $\ell \rightarrow \infty$ in (8), $\lambda \rightarrow 1$. Therefore, if ℓ is chosen to be sufficiently long (relative to θ), then Corollary 4.13 implies that walks with jumps paths with different numbers of jumps have distinct endpoints.

5. A CRITERION FOR HAVING SEPARATE ENDPOINTS

In this section we prove Theorem 1.6 from the introduction. This will require the following trigonometric lemma:

Lemma 5.1. *Let $(o, \mathbf{v}, s, \theta = \pi/2, \ell)$ be the initial data of a walk with jumps having n jumps and burst vector $(1, \dots, 1)$, and number the vertices of the associated walk-with-jumps path p_i and q_i as in Definition 1.3. For any $i < n$ such that $t_{i+1} - t_i \geq R$, the angle η_i measured at the jump endpoint q_i , from the walk axis emanating from q_i to the geodesic arc that joins q_i to the next jump endpoint q_{i+1} satisfies:*

$$\sin \eta_i \leq \frac{\sinh \ell}{\sqrt{\cosh^2(sR) \cosh^2 \ell - 1}}.$$

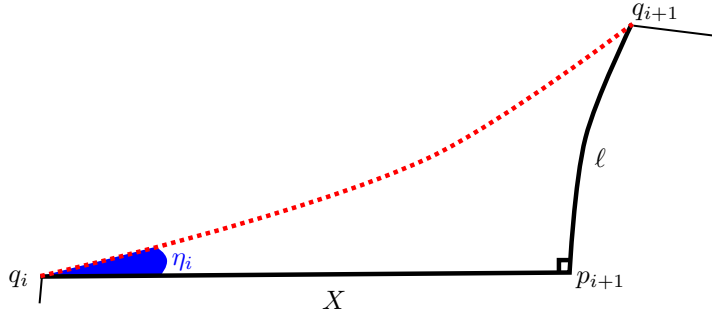


FIGURE 8. A right triangle

Proof. The arcs in question emanating from q_i form a right triangle, together with the $i + 1$ st jump axis, see Figure 8, whose base has length $X = s(t_{i+1} - t_i)$. The length H of the triangle's hypotenuse satisfies $\cosh H = \cosh X \cosh \ell$, by the hyperbolic law of cosines, and by the hyperbolic law of sines the angle η_i satisfies $\sin \eta_i = \sinh \ell / \sinh H$. Rewriting the first formula in terms of $\sinh H$ and substituting into the second yields the one given in the Lemma, but with equality and with X replacing sR . Applying monotonicity of the resulting formula gives the result. \square

We now recall the relevant definitions, also from the Introduction.

Definition 5.2. For $\epsilon > 0$, two walks with jumps sharing initial data and a duration $T > 0$ are *distinct to resolution ϵ* if their sequences of jump times (s_1, \dots, s_m) and (t_1, \dots, t_n) satisfy:

- (1) for each $i \leq \min\{m, n\}$, either $s_i = t_i$ or $|s_i - t_i| > \epsilon$; and
- (2) there exists some i such that $s_i \neq t_i$, or $m \neq n$.

For $R_{\min} > 0$, a walk with jumps has *minimum refractory length R_{\min}* if its burst vector is $(1, \dots, 1)$ —ie. it has no bursts—and for $i \neq j$, $|t_i - t_j| \geq R_{\min}$.

Theorem 1.6. *Given $R_{\min} > 0$, the initial data $(o, \mathbf{v}, s, \theta = \pi/2, \ell)$ of a walk with jumps, and a duration $T > 0$, let*

$$\epsilon = \frac{1}{s} \cosh^{-1} \left(\frac{\cosh(sR_{\min}) + 1}{\cosh(sR_{\min}) - \tanh^2 \ell} \right).$$

Any two walks with jumps having the given initial data, duration T , and minimum refractory length R_{\min} that are distinct to resolution ϵ , have distinct endpoints.

We first prove a special case of Theorem 1.6, from which the general result will follow. It refers to the *walk-with-jumps paths* from Definition 1.3.

Lemma 5.3. *Let $R_{\min} > 0$, the initial data $(o, \mathbf{v}, s, \theta = \pi/2, \ell)$ of a walk with jumps, and a duration $T > 0$ be given, and define ϵ as in Theorem 1.6. For a walk with jumps having the given initial data and duration, and minimum refractory length R_{\min} , which is distinct to resolution ϵ from a walk having its first jump at time 0, the former walk's walk-with-jumps path does not intersect the latter walk's second walk axis (from Definition 2.6). In particular, the two walk-with-jumps paths intersect only at o .*

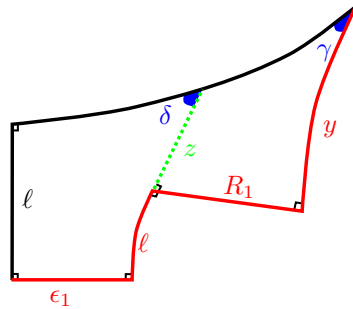


FIGURE 9. A non-convex hexagon.

Proof. Consider two walks-with-jumps having minimum refractory length R_{min} , such that the first has a jump at time 0 and the second has its first jump at time ϵ and its second at time $\epsilon + R_{min}$, the earliest possible. Then the initial segments of their walk-with-jumps paths belong to sides of the hexagon pictured in Figure 9: those of the first belonging to the black sides, and those of the second, the red. Here $\epsilon_1 = s\epsilon$ and $R_1 = sR_{min}$. As in the Figure, we let z be the length of the arc in the second walk's first jump axis joining the endpoint of its first jump segment to the first walk's walk axis. Hyperbolic trigonometry gives the following relations between the lengths of the sides of the resulting "Lambert quadrilateral" (one with three right angles) and the angle δ :

$$\tanh(\ell + z) = \cosh \epsilon_1 \tanh \ell, \quad \text{and} \quad \cos \delta = \sinh \ell \sinh \epsilon_1.$$

As in the proof of Proposition 3.2 we note that if the product $\sinh \ell \sinh \epsilon_1$ were to exceed 1, it would simply mean that the first walk's first walk axis and the second walk's first jump axis did not intersect. This would simultaneously imply that $\cosh \epsilon_1 \tanh \ell > 1$, and hence that the left-hand equation above was also not satisfied.

However we aim to choose ϵ small enough that this does not occur; but large enough that the quantity y of Figure 9 is at least ℓ . To do this we apply angle-sum identities and simplify to solve the left-hand equation above for z :

$$\tanh z = \frac{\cosh \epsilon_1 - 1}{\coth \ell - \tanh \ell \cosh \epsilon_1}.$$

We now observe that since the angle δ is less than $\pi/2$, there is a Lambert quadrilateral contained in the hexagon of Figure 9 that has its side of length R_1 as one side, a side intersecting that with length z , and another side properly contained in the one with length y . Applying the same trigonometric law to this quadrilateral, we obtain:

$$\tanh y \geq \cosh R_1 \tanh z = \frac{\cosh R_1 (\cosh \epsilon_1 - 1)}{\coth \ell - \tanh \ell \cosh \epsilon_1}.$$

Thus to ensure that y is at least ℓ , it is enough to choose ϵ so that the right-hand side above is at least $\tanh \ell$. Setting it equal and solving for ϵ yields the value stated in the theorem.

We note that the right-hand lower bound for y above is increasing in each of ϵ_1 and R_1 . This implies that if the second walk's first jump occurs at a time *at least* the value of ϵ stated in the theorem, then its second jump will not cross the walk axis of the first walk with jumps, since this second jump occurs at a time at least R_{min} after that of the first. We also note that the angle labeled γ in Figure 9, between the first walk's walk axis and the second walk's second jump axis, is less than the angle labeled δ in the figure. This is because the quadrilateral in the figure, with angles γ , $\pi - \delta$, and two right angles, has angle sum less than 2π .

Let q_i be the endpoint of the i th jump of the second walk, and let τ_i be the geodesic ray starting at q_i and passing through q_{i+1} . Since the difference in jump times $t_{i+1} - t_i$ is at least the minimum refractory length R_{min} , and $R_1 = sR_{min}$, Lemma 5.1 asserts that the angle η_i at q_i made by τ_i and the walk axis emanating from q_i satisfies:

$$\sin \eta_i \leq \frac{\sinh \ell}{\sqrt{\cosh^2 R_1 \cosh^2 \ell - 1}}.$$

We claim first that this bound implies that $\eta_i \leq \pi/2 - \delta$; or equivalently, comparing the bound with the formula for $\cos \delta$, that $\sinh \epsilon_1 \sqrt{\cosh^2 R_1 \cosh^2 \ell - 1} \geq 1$. Substituting gives the left-hand side:

$$(9) \quad \sqrt{\left[\left(\frac{\cosh R_1 + 1}{\cosh R_1 - \tanh^2 \ell} \right)^2 - 1 \right] (\cosh^2 R_1 \cosh^2 \ell - 1)}$$

It is a straightforward computation to show that (9) exceeds 1.

We now claim that as a consequence of this, the first and second walks with jumps do not cross.

Let ρ be the walk axis of the first jump in Figure 9 and let λ_i be the i th jump axis of the second walk. We claim that if λ_i intersects ρ , the intersection between λ and ρ in the quadrant bounded by λ and ρ containing o is at an angle $\xi_i \leq \delta$. Indeed, if λ_i does not intersect ρ , then for all $j \geq i$, λ_j does not intersect ρ because λ_i separates λ_j from ρ , by Corollary 4.5. If λ_{i-1} and λ_i intersect ρ , then using the walk axis between λ_{i-1}, λ_i , there is a quadrilateral whose angles are $\pi - \xi_{i-1}, \frac{\pi}{2}, \frac{\pi}{2}$ and ξ_i since the angle sum must be less than 2π , we have $\xi_i \leq \xi_{i-1}$. Since $\xi_1 = \delta$, $\xi_i \leq \delta$ by induction.

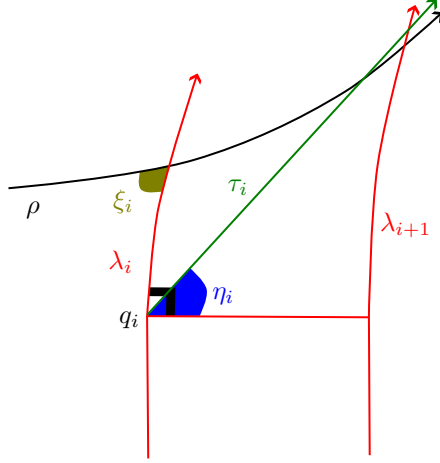


FIGURE 10. The setup for showing that the first and second walk do not intersect.

Aside from its first jump, the first walk travels entirely above ρ , see Corollary 4.5 for details. Therefore, if the first and second walks with jumps cross, the second walk must cross ρ . Since η_i is acute, if q_i sits below ρ , the ray following the walk axis at q_i heading in the direction of travel cannot cross ρ . Thus if the first and second walks with jumps cross, then there exist a pair q_i, q_{i+1} that lie on opposite sides of ρ since the second walk must intersect ρ in a jump. Then τ_i crosses ρ . However we observe that if τ_i and ρ cross, then there would be a triangle formed by ρ, τ_i and λ_i where two of the interior angles are $\frac{\pi}{2} - \eta_i, \pi - \xi_i$. We have $\frac{\pi}{2} - \eta_i \geq \frac{\pi}{2} - (\frac{\pi}{2} - \delta) = \delta$, and $\pi - \xi_i \geq \pi - \delta$, so the interior angle sum of this triangle is at least $\pi - \delta + \delta = \pi$ so the third vertex of this triangle at the intersection of τ_i and ρ must be ideal. Therefore ρ, τ_i do not cross, so the first and second walks with jumps cannot intersect except at o . \square

Theorem 1.6 will now follow directly from the more precise result below.

Theorem 5.4. *Suppose (s_1, \dots, s_m) and (t_1, \dots, t_n) are the jump time sequences of two walks with jumps satisfying the hypotheses of Theorem 1.6. Define*

$$k_0 = \max(\{1\} \cup \{k \mid s_i = t_i \text{ for all } i < k\}),$$

The intersection of the corresponding walk-with-jumps paths is the union of their i^{th} walk and jump segments, for all $i < k_0$, together with the shorter of the two k_0^{th} walk segments.

Proof. If (say) $s_1 = 0$ and $t_1 > 0$ then k_0 defined as above equals 1, the first walk-with-jumps path has a degenerate first walk segment consisting only of the origin o , and the Theorem's conclusion specializes to that of Lemma 5.3. Our goal is to reduce to this case.

Let us assume now that either $m > n$ and $s_i = t_i$ for all $i \leq n$, whence $k_0 = n + 1$, or that $0 < s_{k_0} < t_{k_0}$. Then for the two walk-with-jumps paths, constructed as in Definition 1.3, the points p_i and q_i coincide for all $i < k_0$. Moreover, the k_0^{th} walk segment of the walk with jump times s_i is a subsegment of the other walk's k_0^{th} walk segment. Let γ_{k_0} and λ_{k_0} be the k_0^{th} walk and jump axes, respectively, of the walk with jump times s_i , defined as in 2.6. By Lemma 2.7, these are characterized by containing this walk's respective walk and jump segments. We claim that for the half-planes $H_{k_0-1}^-$ and $K_{k_0}^-$ respectively bounded by these axes, identified in Corollary 4.5, $H_{k_0-1}^- \cap K_{k_0}^-$ contains the union of the segments that were identified above as common to the two walk-with-jumps paths, and the intersection of complementary half-spaces $H_{k_0-1}^+ \cap K_{k_0}^+$ contains the remainder of each of the two walk-with-jumps paths.

Corollary 4.5 asserts in particular that $H_{k_0-1}^-$ contains the duration- s_{k_0-1} initial segment, and $K_{k_0}^-$ the duration- s_{k_0} initial segment, of the walk-with-jumps path corresponding to the walk with jump times s_i . We note that $H_{k_0-1}^-$ also contains this walk's k_0^{th} walk segment, since this segment lies in the bounding geodesic γ_{k_0} . Therefore it contains all of the common segments identified above, and the duration- k_0 initial segment does as well.

The remainder of the walk-with-jumps path corresponding to the walk with jump times s_i , outside the union of its segments in common with the other walk-with-jumps path, consists of the union of its k_0^{th} jump segment with the complement (in the path) of the duration- s_{k_0} initial segment. It is contained in the complement (in the path) of the duration- s_{k_0-1} initial segment, so by Corollary 4.5, it is contained in $H_{k_0-1}^+$. The Corollary moreover asserts that $K_{k_0}^+$ contains the remainder of the path beyond the duration- s_{k_0} initial segment. Since the k_0^{th} jump segment is contained in the bounding geodesic λ_{k_0} of $K_{k_0}^+$, it too contains the entire remainder of the path outside the union of its common segments with the other path.

Turning attention to the walk-with-jumps path corresponding to the walk with jump times t_i , we note that the half-planes $H_{k_0-1}^\pm$ defined for the first path play the same role for this path as for that one: $H_{k_0-1}^-$ contains the union of its duration- t_{k_0-1} initial segment with its k_0^{th} walk segment, and $H_{k_0-1}^+$ contains the complement (in the path) of the duration- t_{k_0-1} initial segment. It follows that $H_{k_0-1}^-$ contains the union of segments that the first path has in common with this one, and that $H_{k_0-1}^+$ contains the complement in this path of that union of segments.

The half-planes $K_{k_0}^\pm$ defined for the first path do not play the same role for this path as for that one; however, their bounding geodesic λ_{k_0} intersects this walk's k_0^{th} walk segment at an angle of θ in its interior, between its points of intersection with this walk's $k_0 - 1^{\text{st}}$ and k_0^{th} jump axes—its endpoints. Arguing as in Lemma 4.1 we therefore find that γ_{k_0} is disjoint from each of these jump axes, so by Corollary 4.5 $K_{k_0}^-$ contains the duration- t_{k_0-1} initial segment and $K_{k_0}^+$ contains the complement (in the path) of the duration- t_{k_0} initial segment. Moreover, γ_{k_0} divides the first walk's k_0^{th} walk segment from its complement in the second walk's k_0^{th} walk segment. Therefore $K_{k_0}^+$ contains the complement in the second walk's walk-with-jumps path of the union of common segments. This establishes the claim's second half.

The claim implies that if the first walk's walk-with-jumps path has a point of intersection with that of the second outside the union of common segments, then this point of intersection must belong to the complement of the union of common segments in the second walk-with-jumps path as well. This is because these complementary sub-paths are walled off from the union of common segments within the quadrant $H_{k_0-1}^+ \cap K_{k_0}^+$. We now observe that these complementary sub-paths are themselves walk-with-jumps paths of two related walks with jumps, to which we will apply Lemma 5.3 to finish the proof.

Let p_{k_0} be as in Definition 1.3 for the first walk's walk-with-jumps path, ie. the terminal point of its k_0^{th} walk segment, and let \mathbf{w} be the outward-pointing tangent vector to the k_0^{th} walk path at p_{k_0} . Then p_{k_0} may be taken as the common origin, and \mathbf{w} the common initial vector, for two walks with jumps that otherwise share the given walks' initial data, each have duration $T - s_{k_0}$, and whose jump times are $(s'_{k_0} = 0, s'_{k_0+1}, \dots, s'_m)$ and (t'_{k_0}, \dots, t'_n) , respectively, where $s'_j = s_j - s_{k_0}$ for $k_0 \leq j \leq m$ and similarly for t'_j . The walk-with-jumps paths associated to these two walks are exactly the portions of the original walks' walk-with-jumps paths complementary to the union of their duration- T_0 initial segments, for all $T_0 < s_{k_0}$. The two new walks satisfy all hypotheses of Lemma 5.3, so that result's conclusion implies that their walk-with-jumps paths intersect only at the origin p_{k_0} . The current result follows. \square

We finally return to the setting of Example 1.11, using Theorem 5.4 to embed a binary tree in \mathbb{H}^2 so that paths in the tree are taken to walk-with-jumps paths.

Corollary 5.5. *For a given $R_{\min} > 0$ and the initial data $(o, \mathbf{v}, s, \theta = \pi/2, \ell)$ of a walk with jumps, define $\epsilon = \epsilon(R_{\min}, s, \ell)$ as in Theorem 1.6, and let $m = \max\{R_{\min}, \epsilon\}$. For a given $n \in \mathbb{N}$ and a binary tree \mathcal{T} with root vertex p_0 , there is an embedding of a finite subtree of \mathcal{T} to \mathbb{H}^2 , taking p_0 to o , with the property that the path in \mathcal{T} encoded by any binary sequence $w = w_1 \dots w_n$ as in Example 1.11 (with each $w_i \in \{0, 1\}$) maps to the walk-with-jumps path of a walk with jumps having the given initial data and duration $T \doteq n \cdot m$, with a jump at time t if and only if $t = (i - 1)m$ for some i such that $w_i = 1$.*

Proof. We recall from Example 1.11 that $w = w_1 \dots w_n$ encodes a path in \mathcal{T} as follows: at the root proceed left if $w_1 = 1$ and right if $w_1 = 0$. At the $(i - 1)$ th vertex of the path, proceed left if $w_i = 1$ or right if $w_i = 0$. We will map this path to the walk-with-jumps path of the walk with the given initial data and jump time sequence $((i_1 - 1)m, \dots, (i_k - 1)m)$, where $i_1 < \dots < i_k$ is the set of $i \in \{1, \dots, n\}$ such that $w_i = 1$.

Note that such a walk has $k+1$ walk segments, where k is the number of indices i such that $w_i = 1$; and for $1 < j \leq k$, the j^{th} walk segment has length $s(i_j - i_{j-1})m$. (And the first has length $s(i_1 - 1)m$, and the last, $s(n - i_k + 1)m$.) The idea is to divide each walk segment into equal-length subsegments of length sm , then map the path encoded by w via a continuous map taking p_0 to o , such that the i^{th} edge of the path in \mathcal{T} maps to one of these subsegments if $w_i = 0$ (ie. $i \neq i_j$ for any $j \leq k$) and to the union of a single jump segment with the subsequent walk sub-segment if $w_i = 1$. We prescribe that each edge of the path in T have length 1 and require the restriction to each edge to have constant speed.

Let \mathcal{T}_0 be the union of the paths in \mathcal{T} encoded by all binary sequences of length n , a finite subtree. There is a well-defined map on \mathcal{T}_0 that restricts on each such path to the one defined in the paragraph above: for any point $p \in \mathcal{T}_0$ there is a unique embedded edge path in \mathcal{T}_0 joining p_0 to p (since \mathcal{T}_0 is a tree), and for any two paths encoded by binary sequences containing this as a sub-path, the maps to the corresponding walk-with-jumps paths agree on the sub-path, by Theorem 5.4 and the canonical nature of the map's construction above.

Note that the walk with jumps corresponding to any path encoded by a binary sequence has minimum refractory length R_{\min} , since $m \geq R_{\min}$. And any two distinct such walks are distinct to resolution ϵ , since $m \geq \epsilon$. It therefore follows again from Theorem 5.4 that the map on \mathcal{T}_0 is an embedding. \square

6. FURTHER QUESTIONS

The above results establish some of the basic features of walks with jumps, but leave open a number of questions of mathematical and biological interest. First, there are a number of natural distances that can be defined on walk-with-jump paths, including the Hausdorff distance between the paths, the \mathbb{H}^2 -distance between their endpoints, and the edit-length distance between their sequences of jump times [19]. The relationship between these distances is at present unclear. Related to this, the structure of the endpoint set for walks with jumps of a fixed duration and number of jumps is not known: it is connected, but its shape remains to be characterized.

6.1. Stability. This subsection describes a hyperbolic-geometric direction for future study. The observation below follows from standard facts:

Proposition 6.1. *Let σ_1, σ_2 be two walks with jumps that satisfy the hypotheses of Proposition 4.11 so that σ_1, σ_2 have the same endpoints. Then there exists $D = D(\ell, \delta_{\pi-\theta})$ so that the Hausdorff between σ_1, σ_2 is bounded above by D .*

Proposition 6.1 follows immediately from Proposition 4.11 and quasigeodesic stability (see [2, Theorem III.H.1.7]). At large scale, Proposition 6.1 supports the heuristic that two walks with jumps that have the same endpoints have similar behavior. Here are two natural questions that we have investigated but do not have clear answers to:

- (1) For what initial data and at what scale is the bound $D = D(\ell, \delta_{\pi-\theta})$ on Hausdorff distance between walks-with-jumps with the same endpoints effective relative the overall length of the associated walks-with-jumps paths? Compounding this problem is the fact that the value D can be hard to estimate. For example, the proof of [2, Theorem III.H.1.7] shows that D exists

and provides an indirect method to compute D but there is no explicit formula for a good estimate.

- (2) Is there a natural way to translate between differences in walk data and Hausdorff distance between two walks with jumps? Could this be used with Proposition 6.1 to distinguish walks with jumps paths from their data?

6.2. Other Directions. Biological considerations suggest other directions for study and extensions. Neural spike trains are often considered to be samples from a point process; it is therefore of interest to determine how the point process model (e.g., Poisson, Poisson with refractory period, Markov, etc.), impacts the distribution of endpoints and the extent to which walks with jumps may cross. Finally, just as the activity of a single neuron can be formalized as a point process, multi-neuronal activity can be formalized as a labeled point process. In analogy with the walk-with-jump model of a single neuron's activity, multineuronal activity could then be modeled as a walk with jumps in a higher-dimensional space, possibly hyperbolic or with hyperbolic subspaces, in which each neuron's activity corresponds to a different kind of jump.

REFERENCES

- [1] D. Aronov and J. D. Victor. Non-euclidean properties of spike train metric spaces. *Phys Rev E Stat Nonlin Soft Matter Phys*, 69(6 Pt 1):061905, 2004.
- [2] Martin R. Bridson and André Haefliger. *Metric spaces of non-positive curvature*, volume 319 of *Grundlehren der Mathematischen Wissenschaften [Fundamental Principles of Mathematical Sciences]*. Springer-Verlag, Berlin, 1999.
- [3] A. M. Derrington, J. Krauskopf, and P. Lennie. Chromatic mechanisms in lateral geniculate nucleus of macaque. *J Physiol*, 357:241–65., 1984.
- [4] Werner Fenchel. *Elementary geometry in hyperbolic space*, volume 11 of *De Gruyter Studies in Mathematics*. Walter de Gruyter & Co., Berlin, 1989. With an editorial by Heinz Bauer.
- [5] J. I. Gold and M. N. Shadlen. The neural basis of decision making. *Annu Rev Neurosci*, 30:535–74, 2007.
- [6] Y. Hasin-Brumshtein, D. Lancet, and T. Olender. Human olfaction: from genomic variation to phenotypic diversity. *Trends Genet*, 25(4):178–84, 2009.
- [7] Allen Hatcher. *Algebraic topology*. Cambridge University Press, Cambridge, 2002.
- [8] J. Hegde. Time course of visual perception: coarse-to-fine processing and beyond. *Prog Neurobiol*, 84(4):405–39, 2008.
- [9] A. L. Jacobs, G. Fridman, R. M. Douglas, N. M. Alam, P. E. Latham, G. T. Prusky, and S. Nirenberg. Ruling out and ruling in neural codes. *Proc Natl Acad Sci U S A*, 106(14):5936–41, 2009.
- [10] B. B. Lee. The evolution of concepts of color vision. *Neurociencias*, 4(4):209–224, 2008.
- [11] John M. Lee. *Introduction to smooth manifolds*, volume 218 of *Graduate Texts in Mathematics*. Springer, New York, second edition, 2013.
- [12] Y. Mochizuki, T. Onaga, H. Shimazaki, T. Shimokawa, Y. Tsubo, R. Kimura, A. Saiki, Y. Sakai, Y. Isomura, S. Fujisawa, K. Shibata, D. Hirai, T. Furuta, T. Kaneko, S. Takahashi, T. Nakazono, S. Ishino, Y. Sakurai, T. Kitsukawa, J. W. Lee, H. Lee, M. W. Jung, C. Babul, P. E. Maldonado, K. Takahashi, F. I. Arce-McShane, C. F. Ross, B. J. Sessle, N. G. Hatsopoulos, T. Brochier, A. Riehle, P. Chorley, S. Grun, H. Nishijo, S. Ichihara-Takeda, S. Funahashi, K. Shima, H. Mushiake, Y. Yamane, H. Tamura, I. Fujita, N. Inaba, K. Kawano, S. Kurkin, K. Fukushima, K. Kurata, M. Taira, K. Tsutsui, T. Ogawa, H. Komatsu, K. Koida, K. Toyama, B. J. Richmond, and S. Shinomoto. Similarity in neuronal firing regimes across mammalian species. *J Neurosci*, 36(21):5736–47, 2016.
- [13] E. Orsingher and A. De Gregorio. Random flights in higher spaces. *J. Theoret. Probab.*, 20(4):769–806, 2007.
- [14] John G. Ratcliffe. *Foundations of hyperbolic manifolds*, volume 149 of *Graduate Texts in Mathematics*. Springer, Cham, [2019] ©2019. Third edition [of 1299730].

- [15] D. S. Reich, F. Mechler, and J. D. Victor. Temporal coding of contrast in primary visual cortex: when, what, and why. *J Neurophysiol*, 85(3):1039–50, 2001.
- [16] B. J. Richmond and L. M. Optican. Temporal encoding of two-dimensional patterns by single units in primate primary visual cortex. ii. information transmission. *J Neurophysiol*, 64(2):370–80, 1990.
- [17] Peter H. Sellers. On the theory and computation of evolutionary distances. *SIAM J. Appl. Math.*, 26:787–793, 1974.
- [18] S. G. Solomon and P. Lennie. The machinery of colour vision. *Nat Rev Neurosci*, 8(4):276–86, 2007.
- [19] J.D. Victor and K.P. Purpura. Metric-space analysis of spike trains: theory, algorithms and application. *Network*, 8:127–164, 1997.
- [20] X. J. Wang. Decision making in recurrent neuronal circuits. *Neuron*, 60(2):215–34, 2008.
- [21] Q. Zaidi, J. Victor, J. McDermott, M. Geffen, S. Bensmaia, and T. A. Cleland. Perceptual spaces: mathematical structures to neural mechanisms. *J Neurosci*, 33(45):17597–602, 2013.
- [22] Y. Zhou, B. H. Smith, and T. O. Sharpee. Hyperbolic geometry of the olfactory space. *Sci Adv*, 4(8):eaq1458, 2018.

DEPARTMENT OF MATHEMATICS, UNIVERSITY OF PITTSBURGH, 301 THACKERAY HALL, PITTSBURGH, PA 15260

Email address: `jdeblois@pitt.edu`

SWARTHMORE COLLEGE, DEPARTMENT OF MATHEMATICS AND STATISTICS, 500 COLLEGE AVE., SWARTHMORE, PA 19081

Email address: `eeinste1@swarthmore.edu`

FEIL FAMILY BRAIN AND MIND RESEARCH INSTITUTE, WEILL CORNELL MEDICINE, NEW YORK, NY 10065

Email address: `jdvicto@med.cornell.edu`